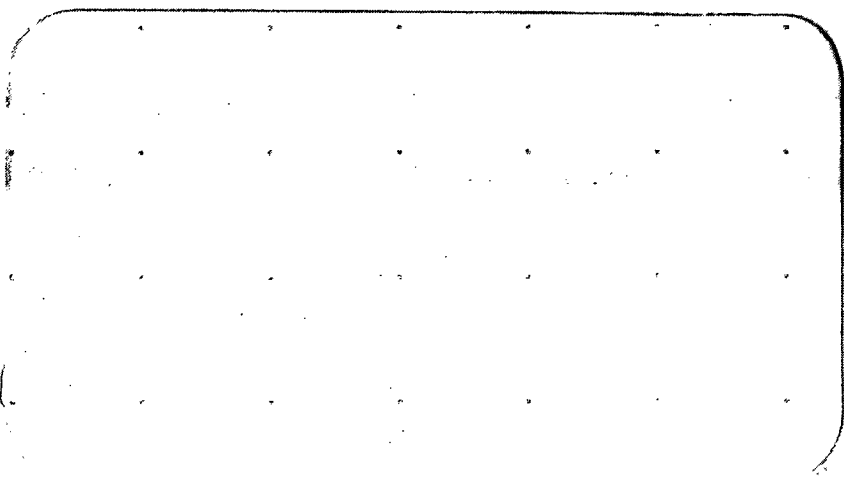


N72-24606

CASE FILE COPY



iiTri

Contract No. NAS8-26791
Report No. IITRI-C6233-12
(Triannual Report)

DEVELOPMENT OF SPACE STABLE THERMAL
CONTROL COATINGS FOR USE ON LARGE
SPACE VEHICLES

National Aeronautics and Space
Administration
George C. Marshall Space Flight Center
Huntsville, Alabama 35812

Prepared by

J.E. Gilligan
R.F. Boutin

with contributions from

R.M. Leas
N.A. Ashford

of

IIT Research Institute
Technology Center
Chicago, Illinois 60616

September 1 through December 31, 1971

Funded under Code 124-09-31-0000-33-1-004-080-2510

FOREWORD

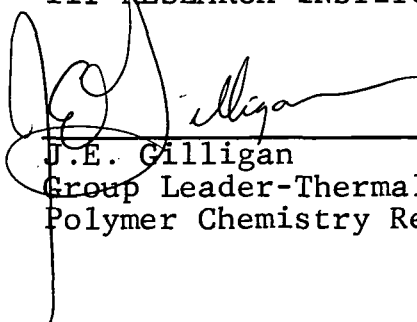
This is Report No. IITRI-C6233-12 (Triannual Report) of IITRI Project C6233, Contract No. NAS8-26791, entitled "Development of Space Stable Thermal Control Coatings for Use on Large Space Vehicles." This report covers the period from September 1 through December 31, 1971.

Major contributors to the program during this period include: Mr. J.E. Gilligan, Project Leader, Mr. Robert F. Boutin, ultra-violet monitor studies, irradiation experiments and reflectance measurements; Dr. Nicholas A. Ashford and Mr. Frank H. Jarke, EPR measurements; solid state consultation, Mr. F.O. Rogers, paint preparation; and Mr. Gene A. Zerlaut, general consultation and administrative management.

The work reported herein was performed under the technical direction of the Space Sciences Laboratory of the George C. Marshall Space Flight Center; Mr. Daniel W. Gates acted as the Project Manager.


This contract was funded under Code 124-09-31-0000-31-1-004-080-2510.

Respectfully submitted,
IIT RESEARCH INSTITUTE



J.E. Gilligan
Group Leader-Thermal Control
Polymer Chemistry Research

APPROVED:



G.A. Zerlaut
Manager
Polymer Chemistry Research

JEG:jss

IIT RESEARCH INSTITUTE

ABSTRACT

Evaluation and environmental testing of zinc orthotitanate pigments and of coatings made from them constitute the bulk of the work accomplished. Electron paramagnetic resonance spectra of these pigments and their precursor compounds have been studied.

A continuing study of the spectral intensity of Mercury-Argon (AH-6) and Mercury-Xenon sources is reported upon. Results of long term Weather-O-Meter testing of commercially-available, strippable, protective coatings are discussed.

TABLE OF CONTENTS

	<u>Page</u>
FOREWORD	ii
ABSTRACT	iii
LIST OF TABLES	v
LIST OF FIGURES	vi
1. INTRODUCTION	1
2. PIGMENT DEVELOPMENT	2
2.1 Introductory Remarks	2
2.2 Electron Paramagnetic Resonance (EPR) Studies	2
3. COMBINED RADIATION ENVIRONMENT TESTS	6
3.1 Combined Radiation Environment Test Data	6
3.2 CREF-5	6
3.3 CREF-6	18
3.4 Solar Simulator Monitoring	33
4. GENERAL COATINGS INVESTIGATIONS	54
4.1 Introductory Remarks	54
4.2 Strippable Prelaunch Protective Coatings	55
4.3 Salt Spray Effects on S-13G	59
4.4 Ultraviolet Stability of Low Outgassing S-13G	61
REFERENCES	64

LIST OF TABLES

<u>Table No.</u>		<u>Page</u>
1	COMPARISON OF EPR CENTERS IN ZINC ORTHOTITANATE: PIGMENT VS OWENS-ILLINOIS PAINT	4
2	RESULTS OF CREF-5, COMBINED RADIATION TEST OF ZINC ORTHOTITANATE PAINTS AND OWENS-ILLINOIS GLASS RESIN	7
3	RESULTS OF CREF-6, COMBINED RADIATION TEST OF ZINC ORTHOTITANATE PAINTS	22
4	COMBINED IRRADIATION EFFECTS IN Zn_2TiO_4 : K_2SiF_6 /PS-7	32
5	COMBINED IRRADIATION EFFECTS IN Zn_2TiO_4 : K_2SiO_3 (Plasma)/O-I 650	32
6	ULTRAVIOLET-INDUCED CHANGES IN SPECTRAL REFLECTANCE OF "PROTECTED" PAINT FILMS	57
7	RESULTS OF SIMULATED SALT SPRAY EXPOSURE EFFECTS ON S-13G UV DEGRADATION	59
8	UV IRRADIATION PERFORMANCE OF "STRIPPED" S-13G	63

LIST OF FIGURES

<u>Figure No.</u>		<u>Page</u>
1	REFLECTANCE SPECTRA OF OWENS-ILLINOIS 650 GLASS RESIN UNPIGMENTED FILM - PROTONS ONLY	9
2	REFLECTANCE SPECTRA OF OWENS-ILLINOIS 650 GLASS RESIN UNPIGMENTED FILM - PROTONS AND ULTRAVIOLET	10
3	REFLECTANCE SPECTRA OF PLASMA ANNEALED, K_2SiO_3 - ENCAPSULATED $Zn_2TiO_4/O-I$ 650 - PROTONS ONLY	11
4	REFLECTANCE SPECTRA OF PLASMA ANNEALED, K_2SiO_3 - ENCAPSULATED $Zn_2TiO_4/O-I$ 650 - PROTONS AND ULTRAVIOLET	12
5	REFLECTANCE SPECTRA OF PLASMA ANNEALED, K_2SiO_3 - ENCAPSULATED $Zn_2TiO_4/O-I$ 650 - ULTRAVIOLET ONLY	13
6	REFLECTANCE SPECTRA OF K_2SiF_6 -ENCAPSULATED $Zn_2TiO_4/PS-7$ - PROTONS ONLY	15
7	REFLECTANCE SPECTRA OF K_2SiF_6 -ENCAPSULATED $Zn_2TiO_4/PS-7$ - PROTONS AND ULTRAVIOLET	16
8	REFLECTANCE SPECTRA OF K_2SiF_6 -ENCAPSULATED $Zn_2TiO_4/PS-7$ - ULTRAVIOLET ONLY	17
9	REFLECTANCE SPECTRA OF $K_4Si_4W_{12}O_{40}$ -ENCAPSULATED $Zn_2TiO_4/PS-7$ - PROTONS ONLY	19
10	REFLECTANCE SPECTRA OF $K_4Si_4W_{12}O_{40}$ -ENCAPSULATED $Zn_2TiO_4/PS-7$ - PROTONS ONLY	20
11	REFLECTANCE SPECTRA OF $K_4Si_4W_{12}O_{40}$ -ENCAPSULATED $Zn_2TiO_4/PS-7$ - ULTRAVIOLET ONLY	21
12	REFLECTANCE SPECTRA OF PLASMA ANNEALED, K_2SiF_6 - ENCAPSULATED $Zn_2TiO_4/O-I$ 650	23
13	REFLECTANCE SPECTRA OF PLASMA ANNEALED, K_2SiF_6 - ENCAPSULATED $Zn_2TiO_4/PS-7$	25
14	REFLECTANCE SPECTRA OF PLASMA ANNEALED, K_2SiF_6 - ENCAPSULATED $Zn_2TiO_4/PS-7$	26
15	REFLECTANCE SPECTRA OF K_2SiO_3 -ENCAPSULATED $Zn_2TiO_4/O-I$ 650	27

<u>Figure No.</u>		<u>Page</u>
16	REFLECTANCE SPECTRA OF K_2SiO_3 -ENCAPSULATED Zn_2TiO_4 /O-I 650	28
17	REFLECTANCE SPECTRA OF PLASMA ANNEALED, K_2SiF_6 -ENCAPSULATED Zn_2TiO_4 /O-I 650-MODIFIED	29
18	REFLECTANCE SPECTRA OF K_2SiF_6 -ENCAPSULATED Zn_2TiO_4 WITH AND WITHOUT PLASMA ANNEALING	31
19	BLOCK DIAGRAM OF SPECTROMETER/DETECTOR ASSEMBLY	36
20	SPECTRAL RESPONSIVITY CURVE (EG&G DATA)	38
21	QUANTUM EFFICIENCY OF SODIUM SALICYLATE	38
22	SPECTRAL FLUORESCENCE INTENSITY OF SODIUM SALICYLATE	38
23	SCHEMATIC OF REFERENCE PHOTODIODE CIRCUITRY	40
24	SCHEMATIC OF PHOTODIODE SENSOR CIRCUITRY	40
25	CHOPPER-DETECTOR ASSEMBLY	41
26	SPECTROMETER AND THE PAR	42
27	EXPERIMENTAL SET-UP	43
28	AH-6 INTENSITY SPECTRUM-MANUFACTURER'S DATA	44
29	SPECTRAL RADIANCE OF NEW HANOVIA 5000W MERCURY-XENON LAMP-MANUFACTURER'S DATA	45
30	AH-6 INTENSITY SPECTRUM - 0 HRS (NEW)	46
31	AH-6 INTENSITY SPECTRUM - 72 HRS	47
32	AH-6 INTENSITY SPECTRUM - 167 HRS	48
33	AH-6 INTENSITY SPECTRA - COMPOSITE	49
34	SPECTRAL RADIANCE OF HANOVIA 5000 WATT MERCURY-XENON LAMP	51
35	RESTART EFFECT ON AH-6 RADIANT OUTPUT	52
36	UV DEGRADATION OF STANDARD AND SALT SPRAY TREATED S-13G	60
37	EFFECT OF UV IRRADIATION ON "STRIPPED" S-13G	62

Report No. IITRI-C6233-12
(Triannual Report)

DEVELOPMENT OF SPACE STABLE THERMAL
CONTROL COATINGS FOR USE ON LARGE SPACE VEHICLES

1. INTRODUCTION

The research effort in passive spacecraft temperature control has, historically, been concentrated on the development of the class of surfaces known as solar reflectors - that is, surfaces with high reflectance for solar radiation and with high emittance in the thermal (infrared) spectrum. The principal requirement of these surfaces is that they be stable in the total environment that they will experience. This requirement means that, once we have achieved a high level of intrinsic stability of these materials in the laboratory, we must be able to produce them in large quantities, and that we must make certain that this stability is preserved in the process and will exist and can be protected in the practical sense as well. Applications on large space vehicles, therefore, present new R&D problems - not simply traditional problems in greater dimensions.

The program consists of four major tasks: pigment development, binder development, environmental effects evaluations, and general coatings investigations. The relative emphasis in each of these tasks varies according to the urgency of the problems elucidated in our investigations, and, of course, with the availability of time and funds. Our efforts have been expended mainly on pigment development, Electron Paramagnetic Resonance (EPR) studies, environmental testing and evaluation activities, and supporting studies. Strippable coatings evaluations and activities of a more general nature were carried out at a comparatively low level of effort.

2. PIGMENT DEVELOPMENT

2.1 Introductory Remarks

The excellent optical properties and stability to ultraviolet radiation exhibited by zinc orthotitanate, Zn_2TiO_4 , (Ref. 1) make it apparent that means to produce this pigment in its most stable form be developed. As we have discussed at length in Reference 2, the stoichiometry of the preparative mixture and the subsequent surface treatment of the powder are highly important with respect to pigment stability. The efforts in this task have involved mainly pigment preparation, and EPR analyses of synthesized pigments.

Our interest in pigments other than zinc orthotitanate has diminished because of the increasing difficulty in justifying "long-shots". We will continue, as time and funding permit, to screen white pigments in the hope of finding one which has a stable, low α_s and requires little or no special treatment to stabilize it against ultraviolet radiation. Since experience, however, dictates that pigment materials are not stable in commercial form, the probability of discovering such a pigment for practical applications is virtually nil. Continuing the screening process, nevertheless, provides many insights regarding the mechanisms of ultraviolet damage.

2.2 Electron Paramagnetic Resonance (EPR) Studies

The use of EPR in our pigment development efforts has been rewarding in two significant ways. It has provided a separate and somewhat independent means of studying fundamental properties of materials. Also, for certain materials, results of EPR studies appear to be correlatable with the optical changes occurring upon irradiation, thus opening up the possibility of directly quantifying radiation-induced optical damage.

The main usefulness of EPR in this program is in the identification and characterization of defects which are environmentally created. Electron paramagnetic resonance information can be very

important also in detecting pigment-vehicle interactions. A primary goal of these studies, however, has been to establish conclusively a quantitative correlation between optical and EPR centers. This goal has been partly met.

2.2.1 Experimental Work

Ultraviolet-irradiations performed at liquid-nitrogen temperatures for short times (~1 hr) yield essentially the same EPR spectra in the Zn_2TiO_4 pigment alone (B-229) as in the Owens-Illinois paint made from that pigment. In the previous Triannual Report an explanation was suggested for the anomaly that while the EPR spectra are the same the optical reflectance spectra were different. The irradiations, we suspected, were too short and, at 77°K, were in fact producing metastable species which were not directly correlated with the optical damage produced by more extensive irradiation.

We extended the longer term irradiations to B-229 zinc orthotitanate in Owens-Illinois 650 vehicle and have obtained the preliminary observations listed in Table 1 - a comparison of the results obtained on the pigment alone (Ref. 3) vs those obtained on an Owens-Illinois paint made from this pigment.

The basic findings in this test are that: Ti^{+3} is produced in much greater concentration in the paint; the Ti^{+3} is mostly (but not entirely) oxygen- or air-bleachable; the Fe^{+++} form of iron, a natural impurity in the pigment, follows a different concentration history when the pigment is irradiated as a paint than when as a pigment alone; and the signal y' responds differently to irradiation in the pigment alone versus that in the paint.

While the correlation of the EPR centers with optical damage is by no means complete, we do feel that differences in the optical spectra of the pigment and paint are explicable in terms of the centers observed.

Table 1

COMPARISON OF EPR CENTERS IN ZINC ORTHOTITANATE: PIGMENT VS OWENS-ILLINOIS PAINT

Treatment	Center	Pigment (B-229)	Owens-Illinois Paint (B-415)
Unirradiated	y'	g ₁ = 1.9555	Slightly less signal asymmetry than in pigment with g = 1.9555
	x Fe ⁺⁺⁺	g ₁₁ = 1.9569 None observed Moderate amount	None observed None observed
1 hr UV-irradiation	y'	Additional UV-created component	Smaller, more symmetrical signal (g = 1.95565)
	x Fe ⁺⁺⁺	None observed Not examined	Moderate amount Moderate amount
4 hrs irradiation	y'	Not examined	Still smaller signal
	x Fe ⁺⁺⁺	Not examined Not examined	Large amount Large amount
20 hrs irradiation	y'	As with 1 hr irradiation	Not much change
	x Fe ⁺⁺⁺	Moderate amount Large amount	Very large amount Small amount
O ₂ bleaching 850 microns	y'	Not examined	Increase in intensity, slightly greater than after 4 hrs irradiation
	x	Not examined	Decrease in intensity, slightly greater than after 4 hrs irradiation
Air bleaching	y'	UV-created component bleached, return to unirradiated spectra	Return of signal asymmetry, g ₁ = 1.9553, g ₁₁ = 1.9567
	x Fe ⁺⁺⁺	No bleaching; moderate amount remains No change; large amount remains	Further bleaching (decrease) to moderate amount Increase to moderate - large amount

2.2.2 Conclusions

From the basic findings noted above we can definitely ascribe the instability of certain zinc orthotitanate pigments to an interaction with the silicone binder. EPR confirms what is observed optically (in the reflectance spectra): the silicone binder apparently predisposes the zinc orthotitanate pigment to semi-bleachable damage at 890-nm, that is, the so-called "belly" damage. This optical bleaching behavior is characteristic: the damage in the 890 nm region oxygen bleaches, but shorter wavelength damage does not.

The fact that two distinctly different Ti^{+++} signals are detected is consistent with the above observation because large band gap semiconductors display strong surface effects. Environmentally created Ti^{+++} may have different electronic environments, wherein it may have different EPR spectra, depending upon where it resides - in the bulk or in the depletion zone (the band bending region).

From the reflectance spectra we have clearly established the fact that the instability resides with the zinc orthotitanate pigment rather than with the O-I 650 vehicle. This interaction has caused catastrophic damage in certain pigments which may not have been completely stabilized by surface treatments. All of the evidence to date thus strengthens the conclusion that the preparative stoichiometry is very important, for two reasons - to regulate the ZnO excess and to control the surface defect density which may be predisposed to the photocreation of Ti^{+++} .

3. COMBINED RADIATION ENVIRONMENT TESTS

The most important, and most meaningful, earth-bound test which can be performed on candidate thermal control materials is irradiation with simulated space radiations. In IITRI's Combined Radiation Environment Facility (CREF) the samples are exposed to simultaneous ultraviolet and proton radiations and the spectral reflectance measurements are made under high vacuum; also, several auxiliary tests can be performed simultaneously (e.g. residual gas analysis). A 5000 watt Hg-Xe source is used for solar simulation. The CREF, which operates at acceleration factors of 4 ultraviolet suns and 4-6 "winds", provides very good simulation, and thus a representative test of the samples. The sample arrangement and irradiation schedules are quite flexible and many combinations are possible. In many instances it is very important to determine the spectral effects of protons alone, of ultraviolet alone, and of both together. Together with O₂ bleaching data this information allows considerable insight into induced defect formation mechanisms and a good indication of overall performance.

3.1 Combined Radiation Environment Test Data

Two irradiation tests in the Combined Radiation Environment Facility (CREF) have been completed and analyzed during this reporting period, CREF-5 and CREF-6

3.2 CREF-5

3.2.1 CREF-5 Results

The test results (solar absorptance values) are listed in Table 2, where, for convenience, the samples are identified by their IITRI batch (code) numbers.

Codes C-067, C-068 and C-070 are paints with encapsulated zinc orthotitanate pigments (originally from IITRI Batch BRZ-229). C-067 is a potassium silicate paint using zinc orthotitanate encapsulated in potassium silicotungstate (K₄Si₄W₁₂O₄₀) and heat treated at 500°C for 7 hrs. C-068 is a potassium silicate paint

Table 2

RESULTS OF CREF-5, COMBINED RADIATION TEST OF
ZINC ORTHOTITANATE PAINTS AND OWENS-ILLINOIS GLASS RESIN

Sample		Solar Absorptance Values			
No.	Code ^a	Initial	p ⁺ only ^b	p ⁺ + UV ^c	UV only ^d
1	C-070	0.194	0.196		
2	OI-650	0.455	0.458		
3	C-068	0.158	0.204		
4	C-067	0.181	0.194		
5	C-070	0.223		0.236	
6	OI-650	0.423		0.431	
7	C-068	0.171		0.227	
8	C-067	0.184		0.229	
9	C-067	0.200			0.231
10	C-068	0.179			0.204
11	C-070	0.286			0.304

^aThe code is explained in the text.

^b1.85 (15) p⁺/cm², no UV.

^c2.00 (15) p⁺/cm² + 1300 ESH (simultaneous)

^d1300 ESH, no p⁺.

using zinc orthotitanate encapsulated in potassium silicofluoride (K₂SiF₆). C-070 is an Owens-Illinois 650 glass resin paint using plasma annealed, potassium silicate encapsulated zinc orthotitanate (SRI No. 10-22.3). OI-650 is a thin film of Owens-Illinois 650 Glass Resin.

3.2.2 Test Sequence

In CREF-5 the following sequence was utilized. After the initial spectral reflectance measurements were made, proton irradiation (1.2 keV), but no ultraviolet irradiation, was initiated exposing samples No.'s 1-4 only, to 1.85×10^{15} p⁺/cm². The spectral reflectance of samples No.'s 1-12 were then measured. Even though the proton beam can "see" only four samples at a time, spectral reflectance measurements were again made of samples No.'s 5-12 to be certain that changes had not occurred in the interim.

The samples were then rotated such that sample No.'s 5-8 were exposed to the proton beam; irradiation of samples No.'s 5-8 with protons and of all samples with concurrent ultraviolet radiation was then initiated. The ultraviolet exposure was 1300 ESH, and the proton exposure was $2.0 \times 10^{15} \text{ p}^+/\text{cm}^2$ (to samples No.'s 5-8). Spectral reflectance measurements were then made of sample No.'s 5-12; no further measurements of sample No.'s 1-4 were performed.

3.2.3 Discussion of CREF-5 Results

3.2.3.1 Owens-Illinois 650 Glass Resin

Two samples of Owens-Illinois 650 Glass Resin (O-I 650) were tested. The reflectance spectra for a sample which was exposed to protons only is shown in Figure 1. Although solar absorptance is not a completely valid measure of degradation in this case, the $\Delta\alpha_s$ of 0.003 (α_s : 0.455 to 0.458) indicates excellent stability. Note that the damage occurs mainly in the ultraviolet and infrared regions of the spectrum. In Figure 2, the O-I 650 film has been exposed to both proton and ultraviolet radiations. The spectral changes here too are very small and occur in the same spectral regions as for the proton-only sample. The change in α_s is from 0.423 to 0.431; ($\Delta\alpha_s = 0.008$). This behavior suggests that O-I 650 is indeed a very stable binder material and that it is probably more affected by ultraviolet radiation than by protons.

3.2.3.2 Plasma-Annealed, Potassium Silicate-Encapsulated Zinc Orthotitanate in O-I 650; $\text{Zn}_2\text{TiO}_4:\text{K}_2\text{SiO}_3$ (Plasma)/O-I 650

This paint was prepared as IITRI Batch No. C-070 from a plasma-annealed pigment (designated SRI #10-22.3 by Stanford Research Institute). The spectra, taken before and after an exposure to protons only are shown in Figure 3 and indicate that both the pigment and paint are stable to protons. Figure 4 shows the spectra for a paint irradiated with simultaneous proton and ultraviolet radiations, while those in Figure 5 represent ultraviolet effects only. The $\Delta\alpha_s$ values for samples irradiated with

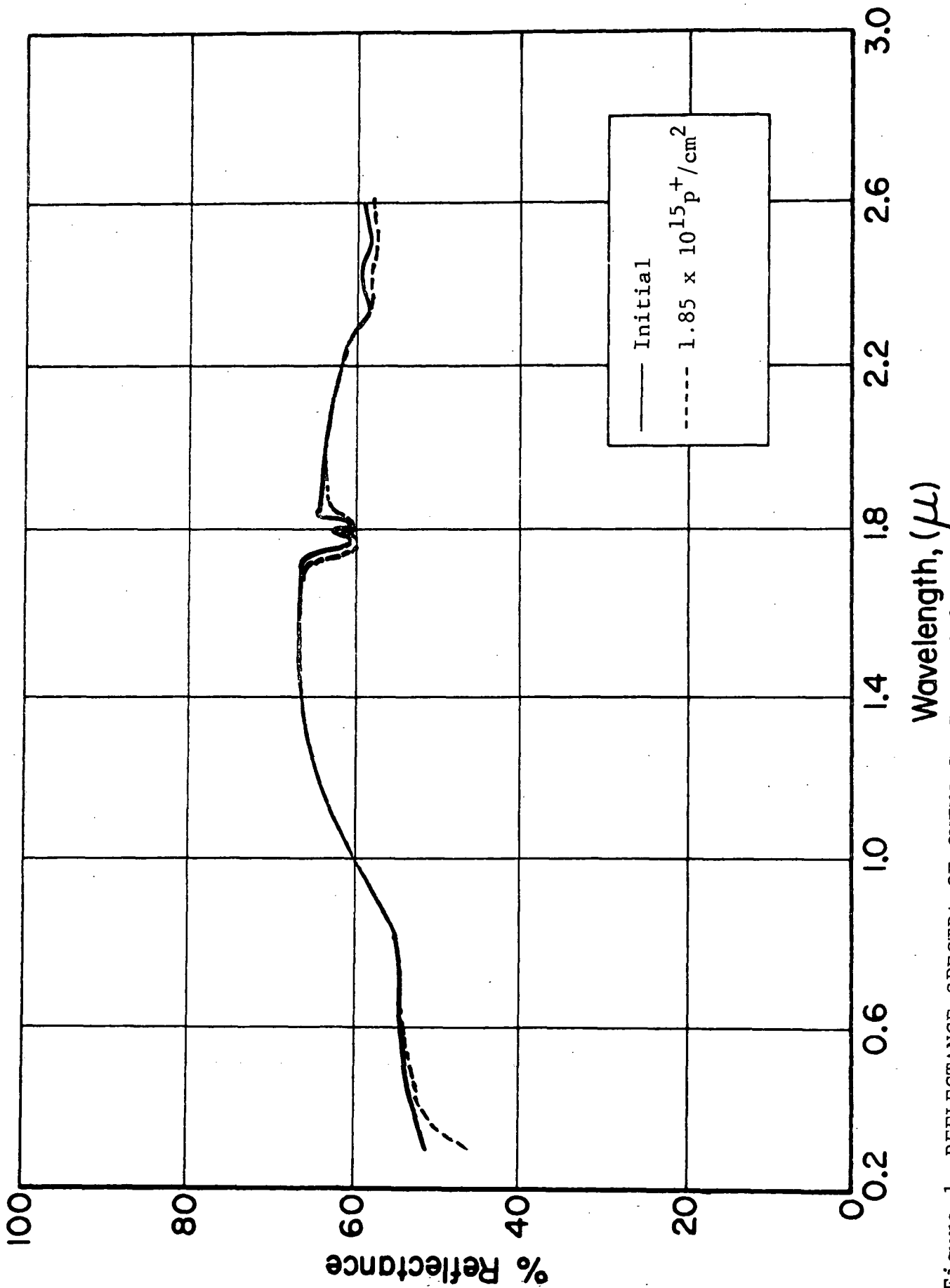


Figure 1 REFLECTANCE SPECTRA OF OWENS-ILLINOIS 650 GLASS RESIN UNPIGMENTED FILM - PROTONS ONLY

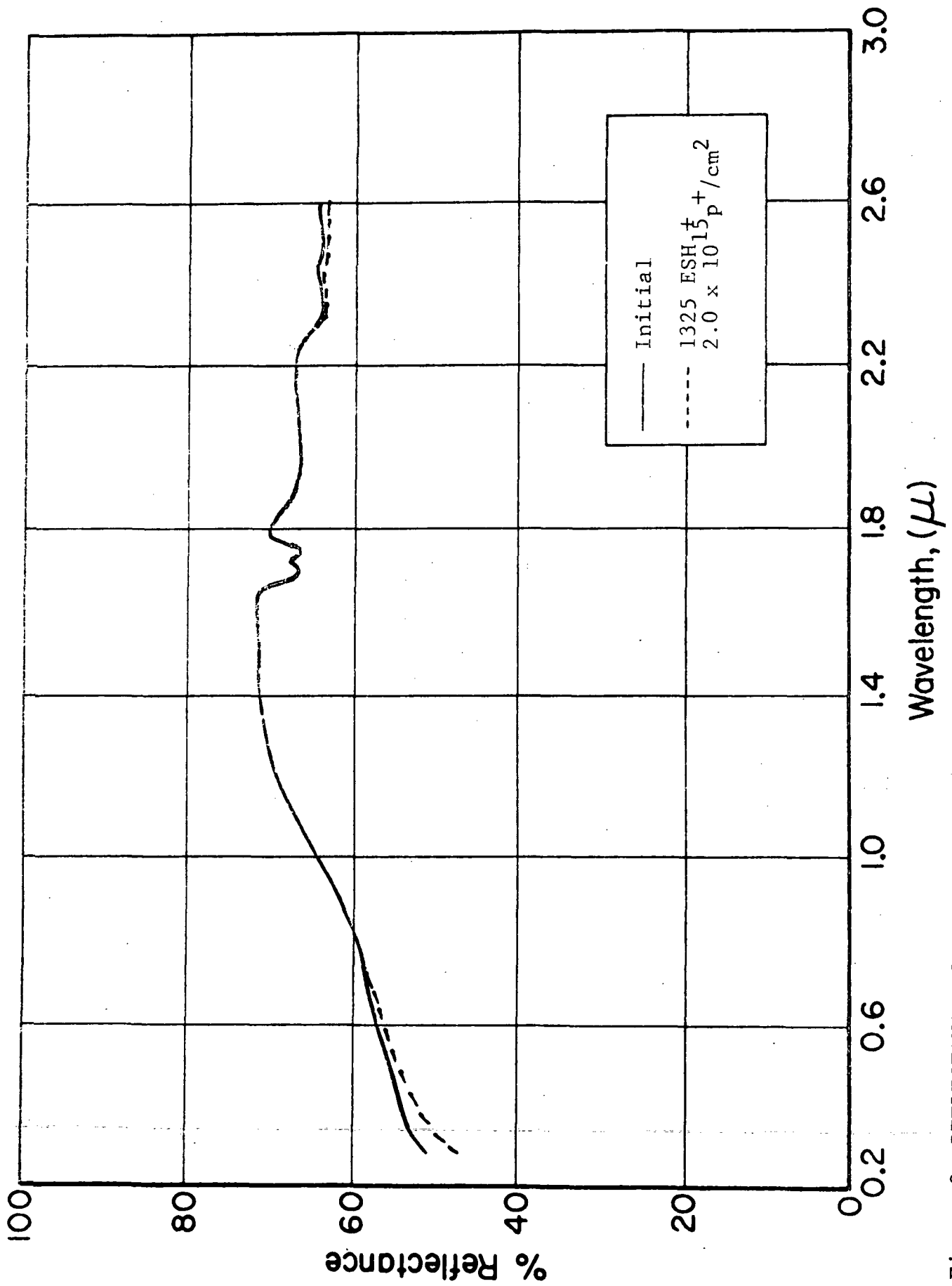


Figure 2. REFLECTANCE SPECTRA OF OWENS-ILLINOIS 650 GLASS RESIN UNPIGMENTED FILM - PROTONS AND ULTRAVIOLET

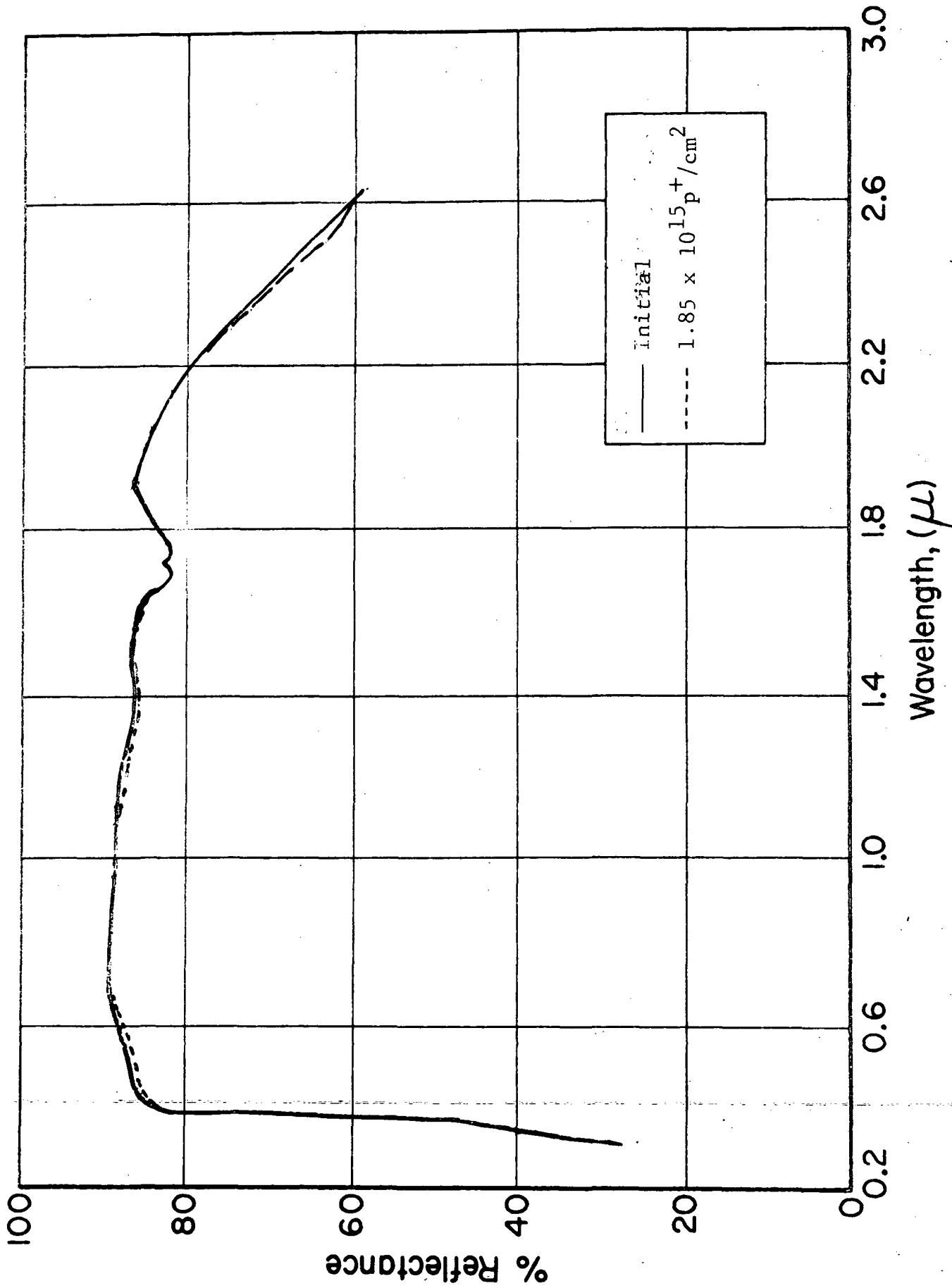


Figure 3 REFLECTANCE SPECTRA OF PLASMA ANNEALED, K_2SiO_3 -ENCAPSULATED Zn_2TiO_4 /O-I 650 - PROTONS ONLY

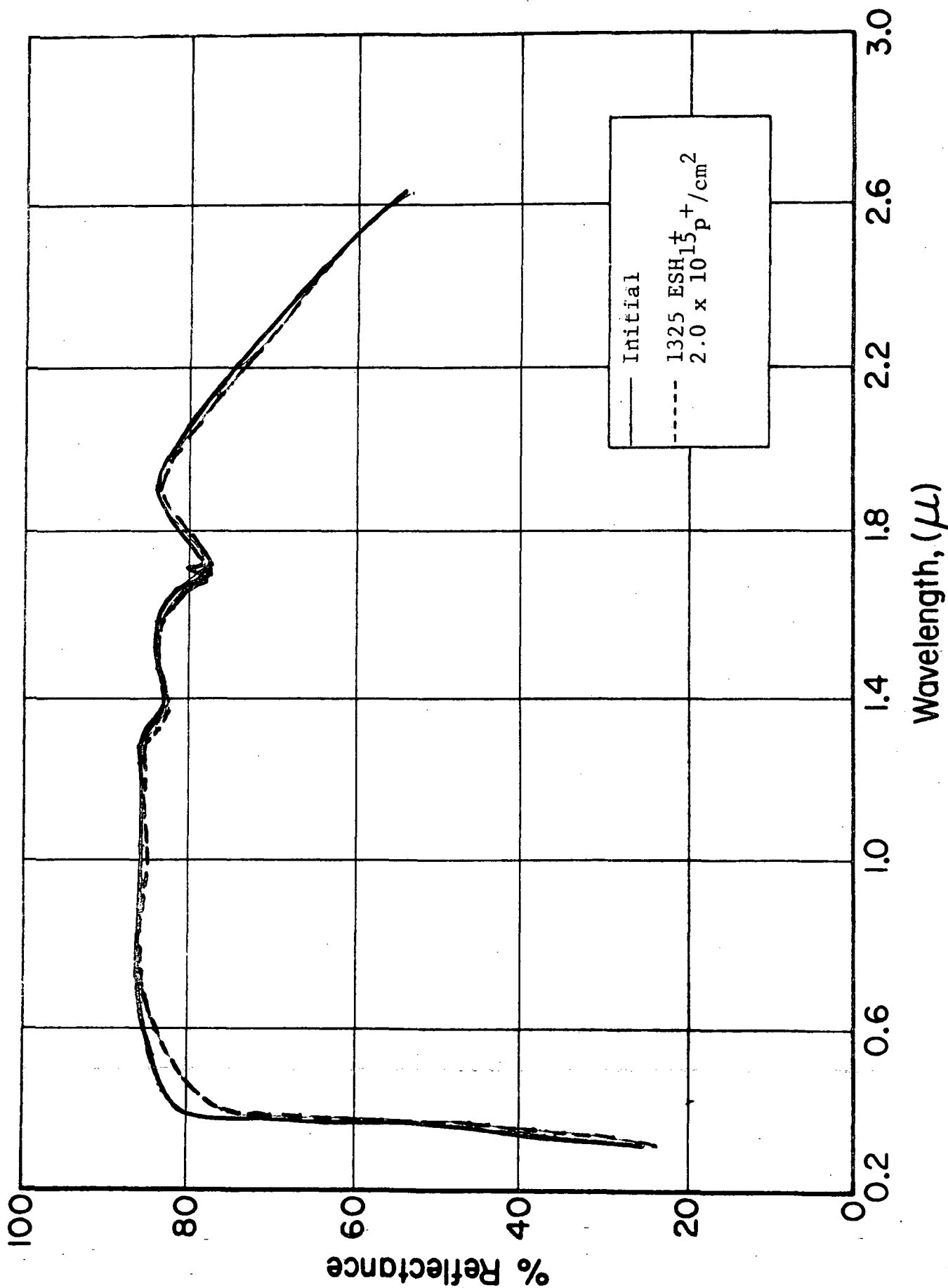


Figure 4 REFLECTANCE SPECTRA OF PLASMA ANNEALED, K₂SiO₃-ENCAPSULATED Zn₂TiO₄/0-I 650 - PROTONS AND ULTRAVIOLET

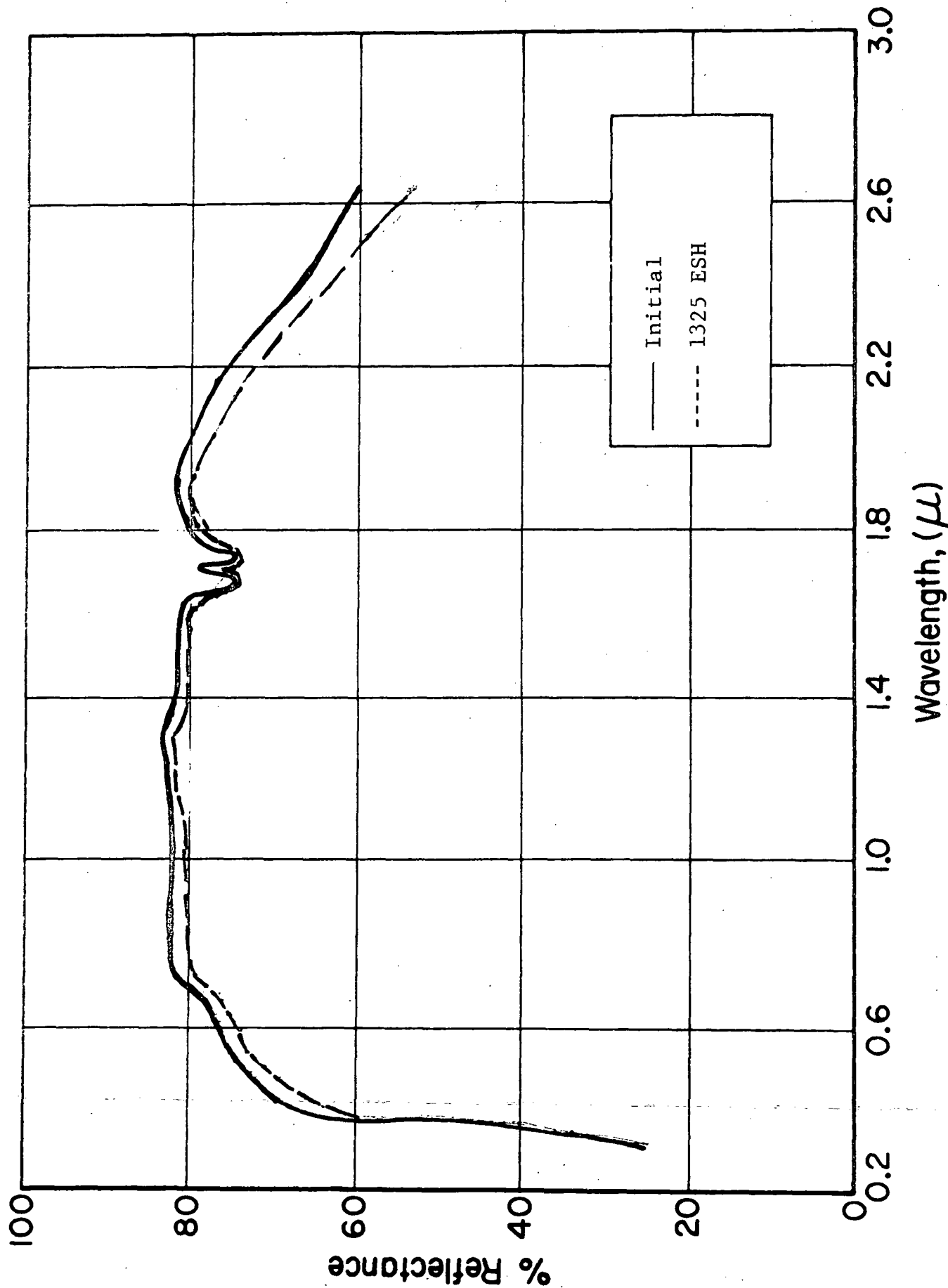


Figure 5 REFLECTANCE SPECTRA OF PLASMA ANNEALED, K_2SiO_3 -ENCAPSULATED $Zn_2TiO_4/O-I$ 650 - ULTRAVIOLET ONLY

protons only (Figure 3), protons plus ultraviolet (Figure 4), and ultraviolet only (Figure 5), are 0.002, 0.013 and 0.018 respectively. From Figure 3 it is evident that protons have a negligible effect. The behavior indicated in Figures 4 and 5, however, is anomalous. Figure 5 shows considerable infrared damage, similar to ZnO degradation, as a result of an ultraviolet exposure, while as Figure 4 shows, a combined exposure produces slightly more overall damage, yet insignificant infrared damage. The somewhat greater degradation of the ultraviolet-irradiated paint compared to that of the same paint irradiated simultaneously with protons and ultraviolet radiation, suggests proton-induced bleaching of ultraviolet-created defects. It is possible also that this latter sample received some spillover from the proton beam during the first (proton only) part of the test. In any event, the performance of this paint system is very good - a nominal degradation of 0.015 after an exposure equivalent to that of approximately 0.25 year in space (based on full solar wind exposure and half-time solar electromagnetic exposure).

3.2.3.3 Potassium Silicofluoride Encapsulated Zinc Ortho- titanate in PS-7; $Zn_2TiO_4:K_2SiF_6/PS-7$

This paint was prepared as IITRI Batch No. C-068; the pigment was not plasma-annealed. Figures 6-8 present the spectra for samples irradiated with protons only (Figure 6), concurrent proton plus ultraviolet (Figure 7), and ultraviolet-only (Figure 8), with $\Delta\alpha_s$ values of 0.046, 0.056 and 0.025, respectively. The sensitivity to protons versus that to ultraviolet is apparently the converse of that of the previous paint system: proton damage exceeds ultraviolet damage. (A similarity to the $Zn_2TiO_4;K_2SiO_3$ (Plasma)/O-I 650 exists in the ZnO-like infrared damage due to ultraviolet.) The overall performance of this pigment, however, compared to other encapsulated pigment materials, is not satisfactory.

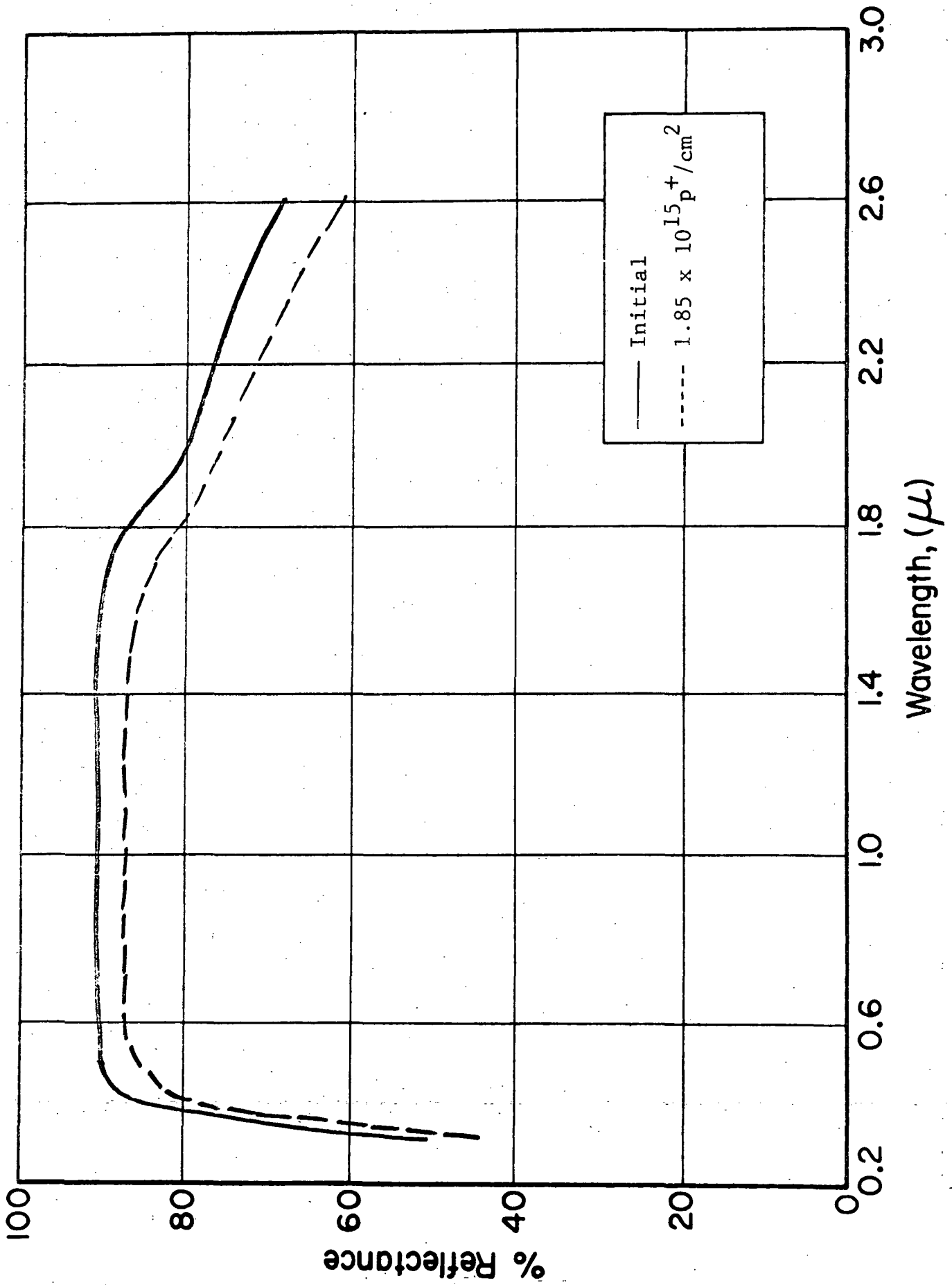


Figure 6 REFLECTANCE SPECTRA OF K_2SiF_6 -ENCAPSULATED $Zn_2TiO_4/PS-7$ - PROTONS ONLY

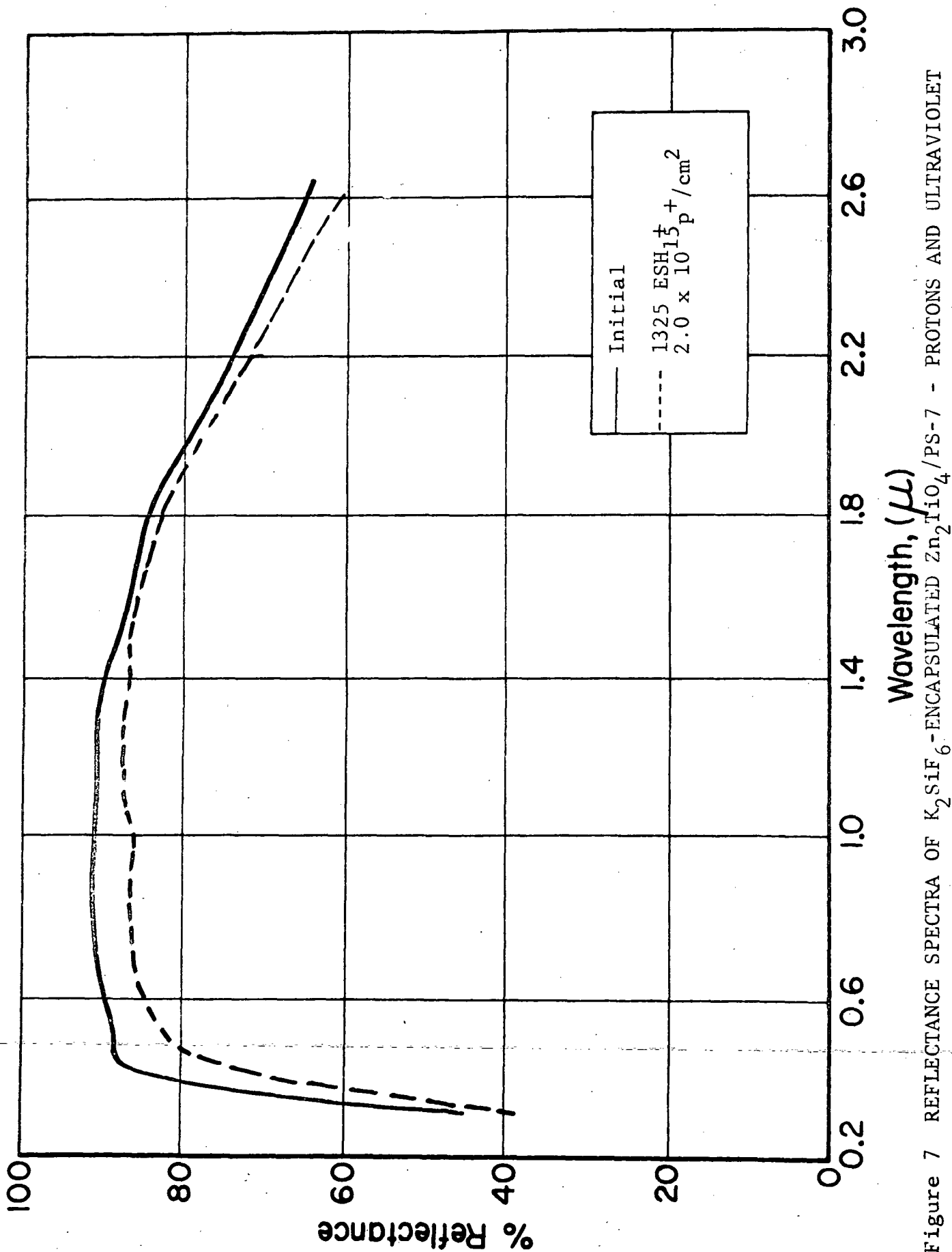


Figure 7 REFLECTANCE SPECTRA OF K_2SiF_6 -ENCAPSULATED $\text{ZnTiO}_4/\text{PS-7}$ - PROTONS AND ULTRAVIOLET

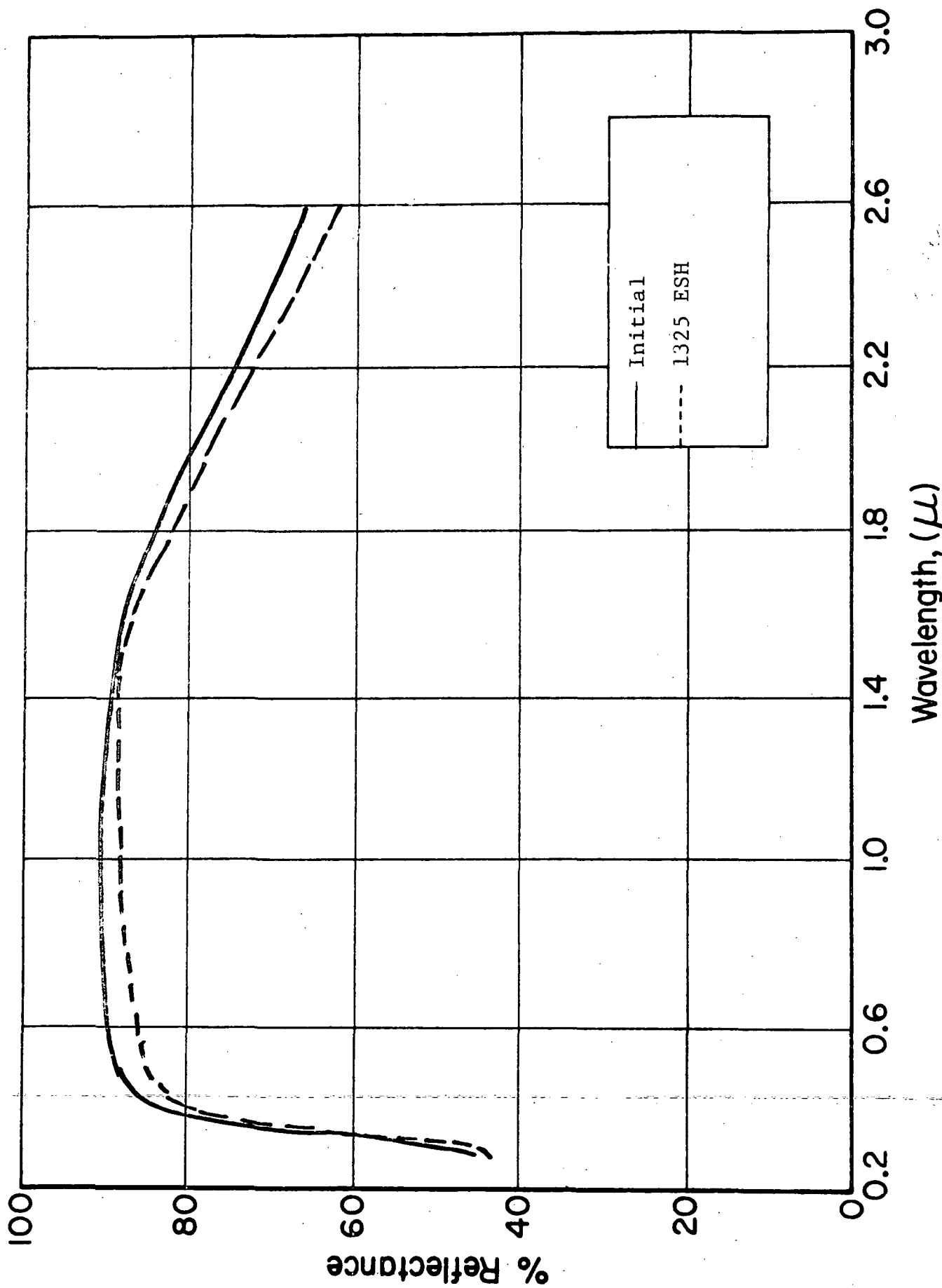


Figure 8 REFLECTANCE SPECTRA OF K_2SiF_6 -ENCAPSULATED $Zn_2TiO_4/PS-7$ - ULTRAVIOLET ONLY

3.2.3.4 Potassium Silicotungstate Encapsulated Zinc Orthotitanate in PS-7; $Zn_2TiO_4:K_4Si_4W_{12}O_{40}/PS-7$

This paint was prepared using potassium silicate (Sylvania Electric Co.'s PS-7) as the vehicle; the pigment was not plasma annealed. The spectral reflectance before and after irradiation are presented in Figures 9-11. As in the case of $Zn_2TiO_4:K_2SiF_6/PS-7$, the effect of concurrent (protons plus ultraviolet) irradiations is greater than that of the individual radiations. Proton irradiation caused the least damage (Figure 9), ($\Delta\alpha_s = 0.013$); in combined proton and ultraviolet radiation the $\Delta\alpha_s$ was 0.045 (Figure 10); and ultraviolet effects produced a $\Delta\alpha_s$ of 0.031. The spectral damage in all cases is generally small and equally distributed over the entire spectrum, although ZnO-like infrared absorption appears more prominent after ultraviolet irradiation. The performance of the silicotungstate-encapsulated Zn_2TiO_4 pigments is somewhat inferior in stability to those encapsulated in potassium silicofluoride.

3.3 CREF-6

3.3.1 Results

In Table 3 below are the solar absorptance values from the CREF-6 test. These data show excellent stability of paints prepared from plasma calcined pigments. It is interesting to note that O-I 650 is apparently more stable than potassium silicate.

The SRI codes refer to paint made from a potassium silicofluoride treated zinc orthotitanate which has been plasma calcined at SRI. SRI-1 is an Owens-Illinois 650 glass resin paint of that pigment; SRI-2, a potassium silicate paint; and SRI-3, a paint prepared from a "modified" O-I 650. C-169 is identical to C-070 (in CREF-5) - an SRI plasma calcined, potassium silicate encapsulated zinc orthotitanate pigment in O-I 650. The solar absorptance values are higher than normal because thin coatings were used in order to avoid stress cracking of the dried films.

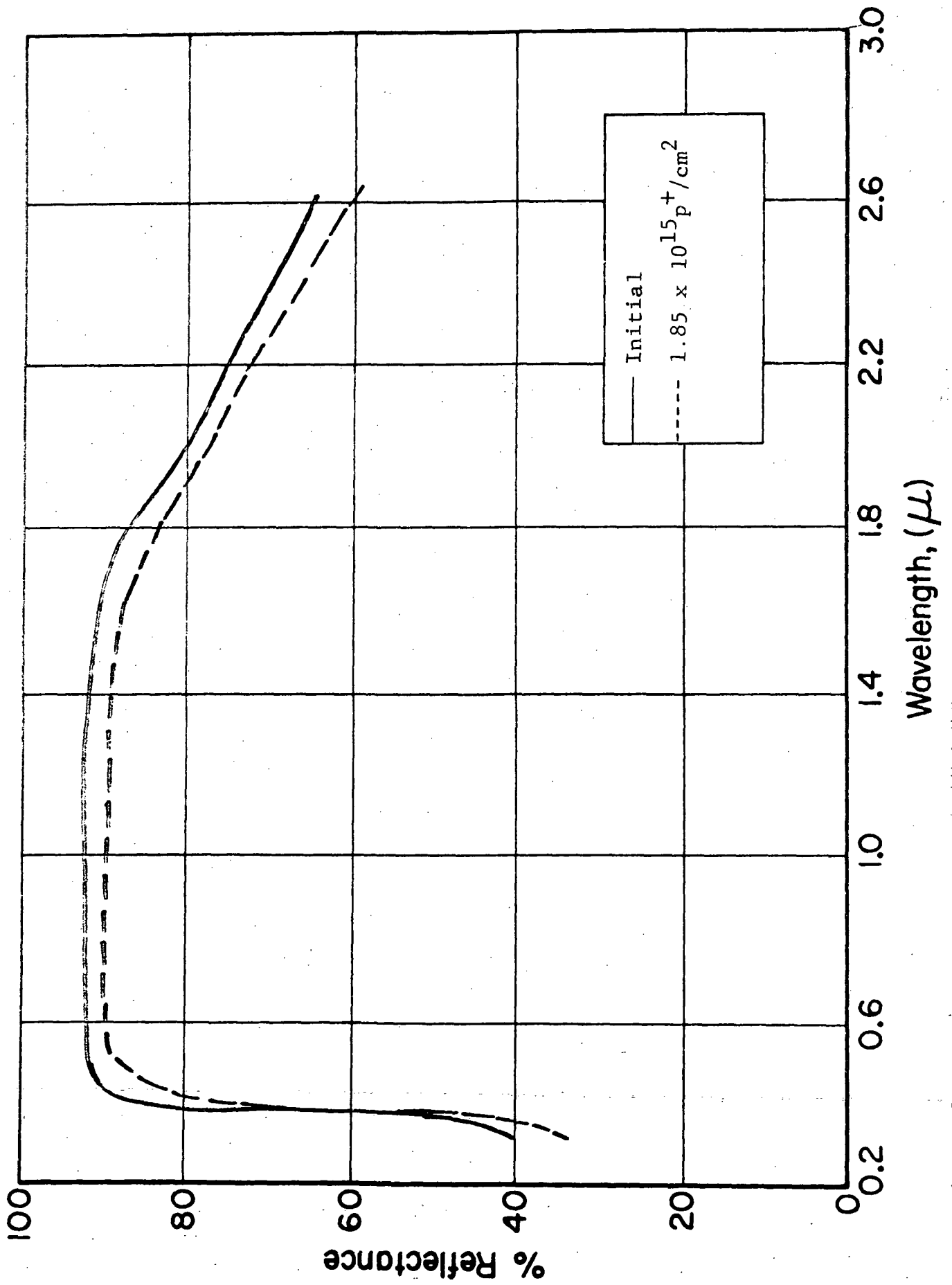


Figure 9 REFLECTANCE SPECTRA OF $K_4Si_4W_{12}O_{40}$ -ENCAPSULATED $Zn_2TiO_4/PS-7$ - PROTONS ONLY

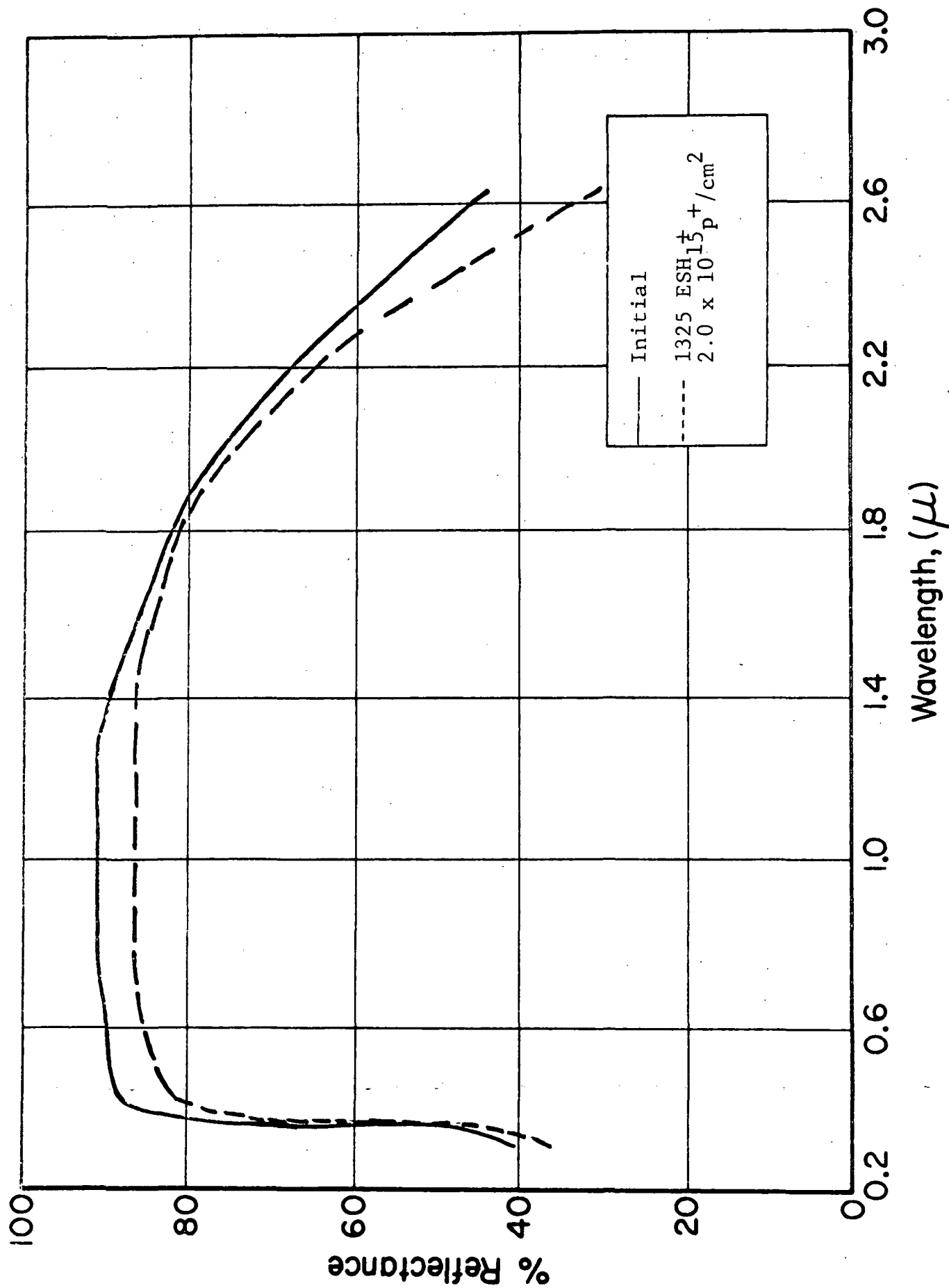


Figure 10 REFLECTANCE SPECTRA OF $K_4Si_4W_{12}O_{40}$ -ENCAPSULATED $Zn_2TiO_4/PS-7$ - PROTONS AND ULTRAVIOLET

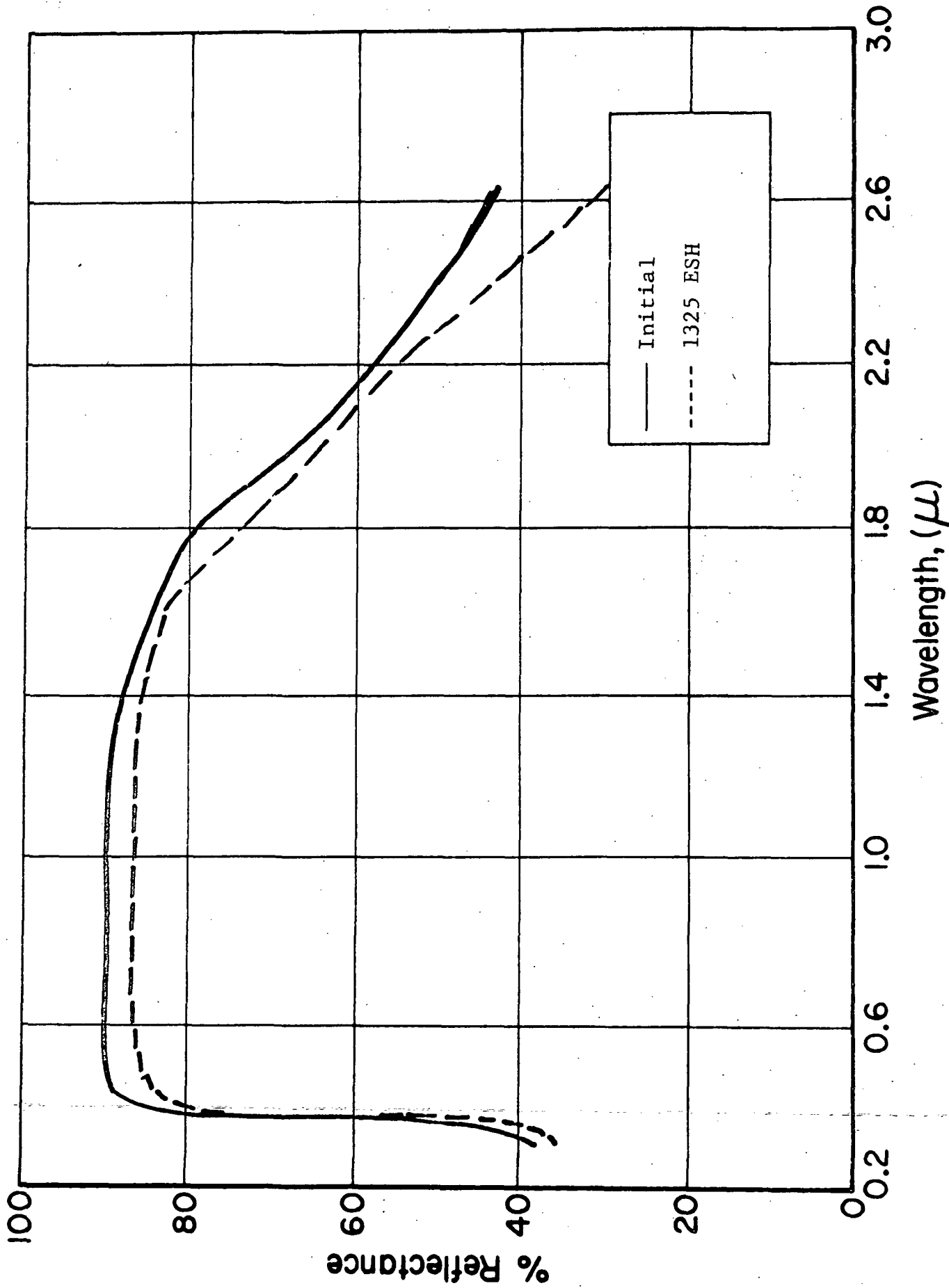


Figure 11 REFLECTANCE SPECTRA OF $K_4Si_4W_{12}O_{40}$ -ENCAPSULATED $Zn_2TiO_4/PS-7$ - ULTRAVIOLET ONLY

Table 3

RESULTS OF CREF-6, COMBINED RADIATION TEST OF
ZINC ORTHOTITANATE PAINTS

Sample		Solar Absorptances				
No.	Code ^a	Initial	(UV + p ⁺) ₁ ^b	(UV + p ⁺) ₂ ^c	UV ₁ -	UV ₂ -
2	SRI-1	0.284	0.301	0.303		
3	C-169	0.290	0.303	0.315		
6	SRI-2	0.251			0.281	0.286
9	SRI-1	0.286			0.305	0.311
11	C-169	0.243			0.252	0.260
12	SRI-3	0.267			0.272	0.280

^aSee text for code explanation.

^b(p⁺ + UV)₁ = 2.44 (15) p⁺/cm² and 1240 ESH.

^c(p⁺ + UV)₂ = 9.61 (15) p⁺/cm² and 2250 ESH.

3.3.2 Test Sequence

A simple sequence of combined radiations was employed in this test. The proton and ultraviolet radiations were simultaneous. The samples were not rotated, so that samples No.'s 2 and 3 were exposed to proton and ultraviolet radiations while the others were exposed only to ultraviolet radiation. Spectral reflectance measurements were made after a combined exposure of 2.44×10^{15} p⁺/cm² and 1240 ESH, and at the end of the test after a cumulative, combined exposure of 9.6×10^{15} p⁺/cm² and 2250 ESH.

3.3.3 Discussion of CREF-6 Results

3.3.3.1 Plasma-Annealed, Potassium Silicofluoride-Encapsulated Zinc Orthotitanate in PS-7; Zn₂TiO₄:K₂SiF₆ (Plasma)/PS-7

The reflectance spectra of this material, which was prepared using a pigment identified as SRI #12-31.3, are presented in Figure 12. The sample was exposed to ultraviolet radiation only. The α_s value degraded 0.030 in the first part of the test, and an additional 0.005 in the second.

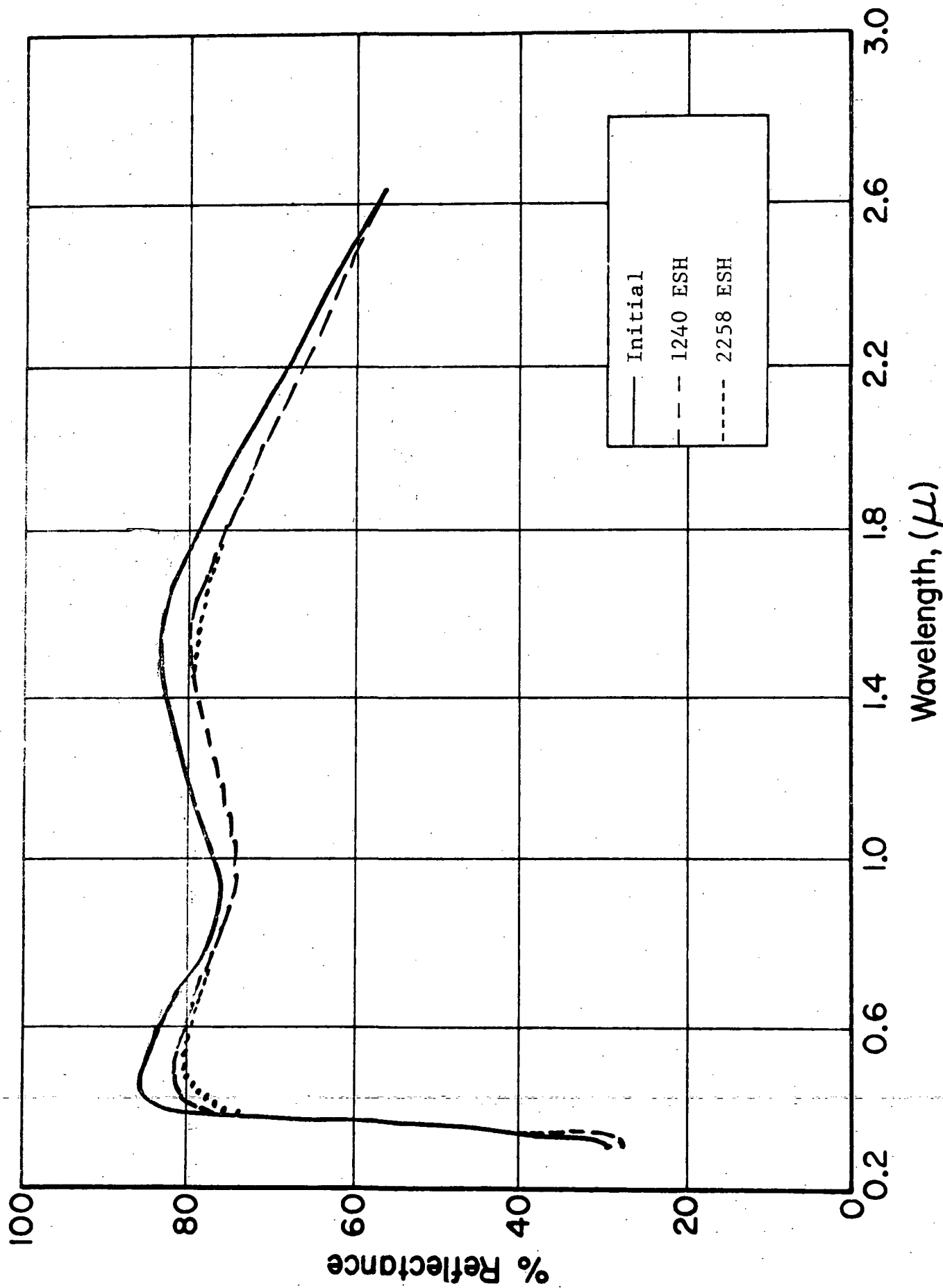


Figure 12 REFLECTANCE SPECTRA OF PLASMA ANNEALED, K_2SiF_6 -ENCAPSULATED Zn_2TiO_4/O_2-I 650

3.3.3.2 Plasma-Annealed, Potassium Silicofluoride-Encapsulated Zinc Orthotitanate in O-I 650; $Zn_2TiO_4:K_2SiF_6$ (Plasma)/O-I 650

For this particular test three O-I 650 paints were prepared; two using standard O-I 650; the third using "modified" (internally plasticized) O-I 650, designated O-I 650-G. One sample was exposed to proton and ultraviolet radiations (Figure 13), and the other two (Figures 14 and 15) including the O-I 650-G paint were exposed to ultraviolet radiation only. The α_s value for the paint (with the standard vehicle) exposed to the combined environment degraded 0.017 in the first part of the test and an additional 0.002 in the second. The α_s value for the "standard" paint exposed to ultraviolet radiation only degraded 0.019 in the first part of the test and an additional 0.006 in the second. The stability of the "modified" paint is considerably better; α_s increased only 0.005 in the first part; an additional 0.008 in the second. All these changes are well within experimental error, and hence not necessarily indicative of a trend. In any event the stability of this paint system is exceptionally good.

3.3.3.3 Plasma-Annealed, Potassium Silicate-Encapsulated Zinc Orthotitanate in O-I 650; $Zn_2TiO_4:K_2SiO_3$ (Plasma)/O-I 650

This paint was prepared as IITRI Batch No. C-169 and is identical, except in date of preparation, with IITRI Batch No. C-070, evaluated in CREF-5. The reflectance spectra for the two samples irradiated with ultraviolet radiation only are given in Figures 16 and 17. The α_s value of the sample whose spectra are shown in Figure 16 degraded 0.013 in the first part, and 0.012 in the second. In the case of the other ultraviolet-only sample (Figure 17), α_s degraded 0.009 in the first part and an additional 0.008 in the second. Within experimental error, these are consistent results.

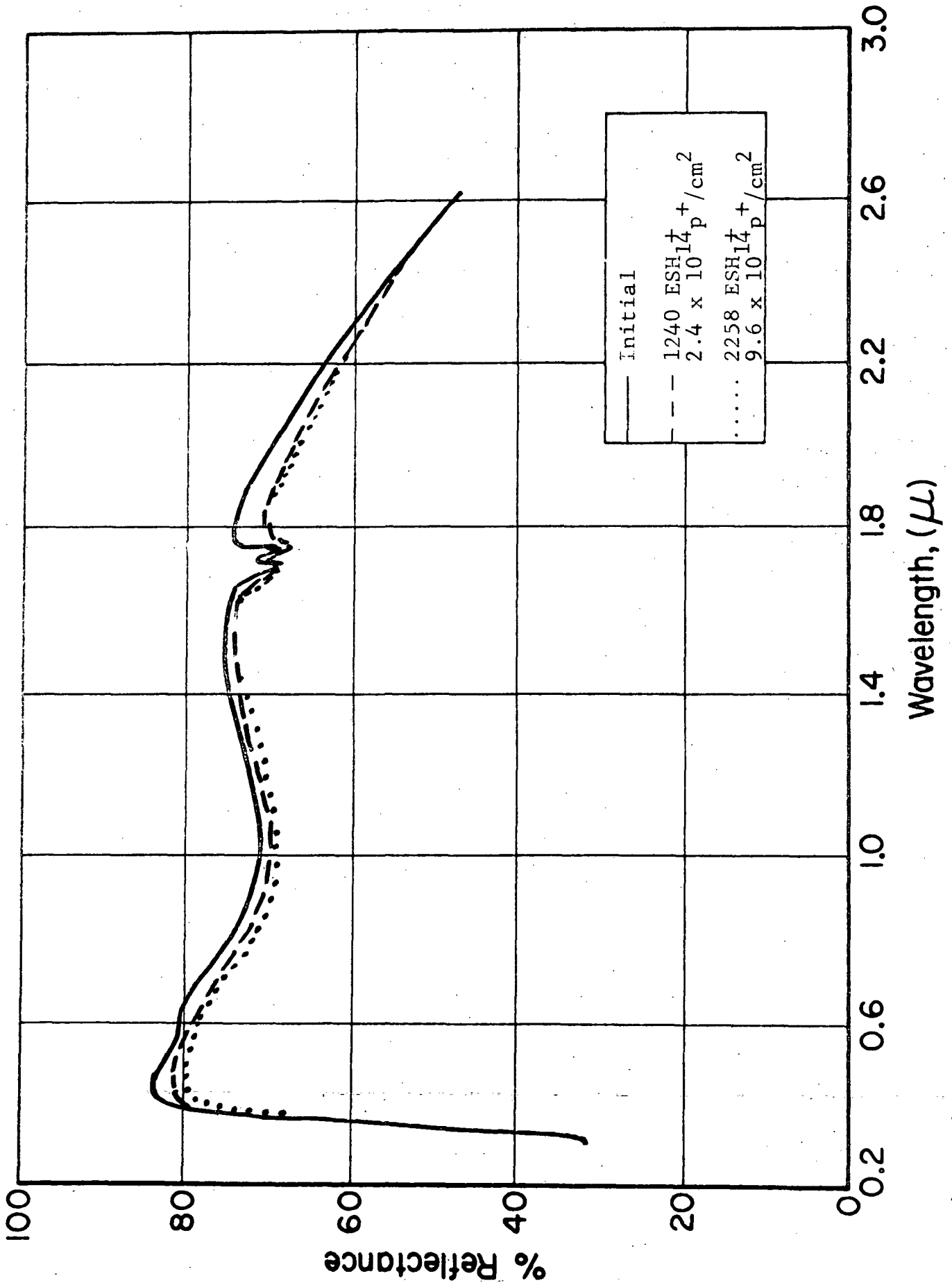


Figure 13 REFLECTANCE SPECTRA OF PLASMA ANNEALED, K_2SiF_6 -ENCAPSULATED $Zn_2TiO_4/PS-7$

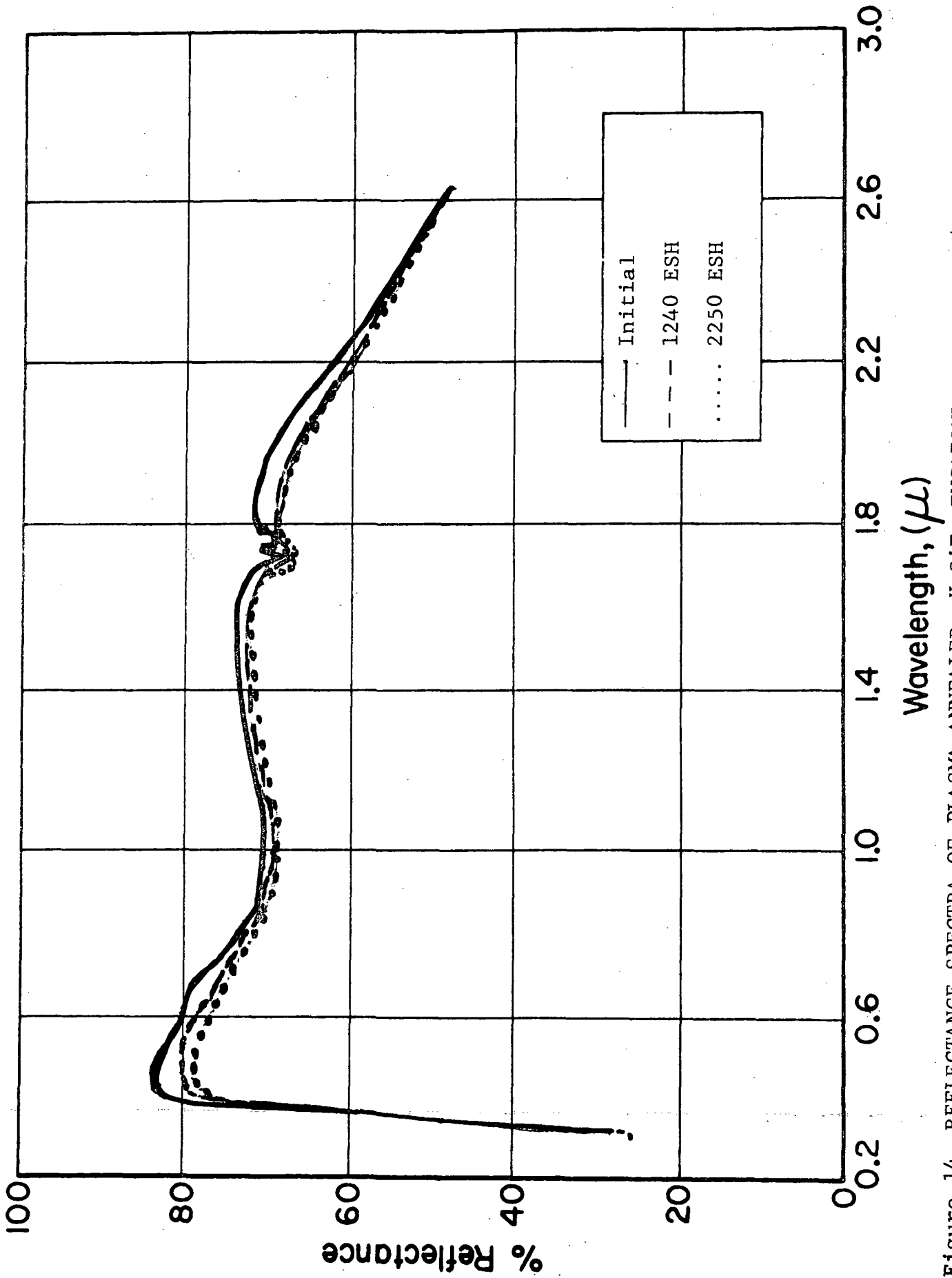


Figure 14 REFLECTANCE SPECTRA OF PLASMA ANNEALED, K_2SiF_6 -ENCAPSULATED $Zn_2TiO_4/PS-7$

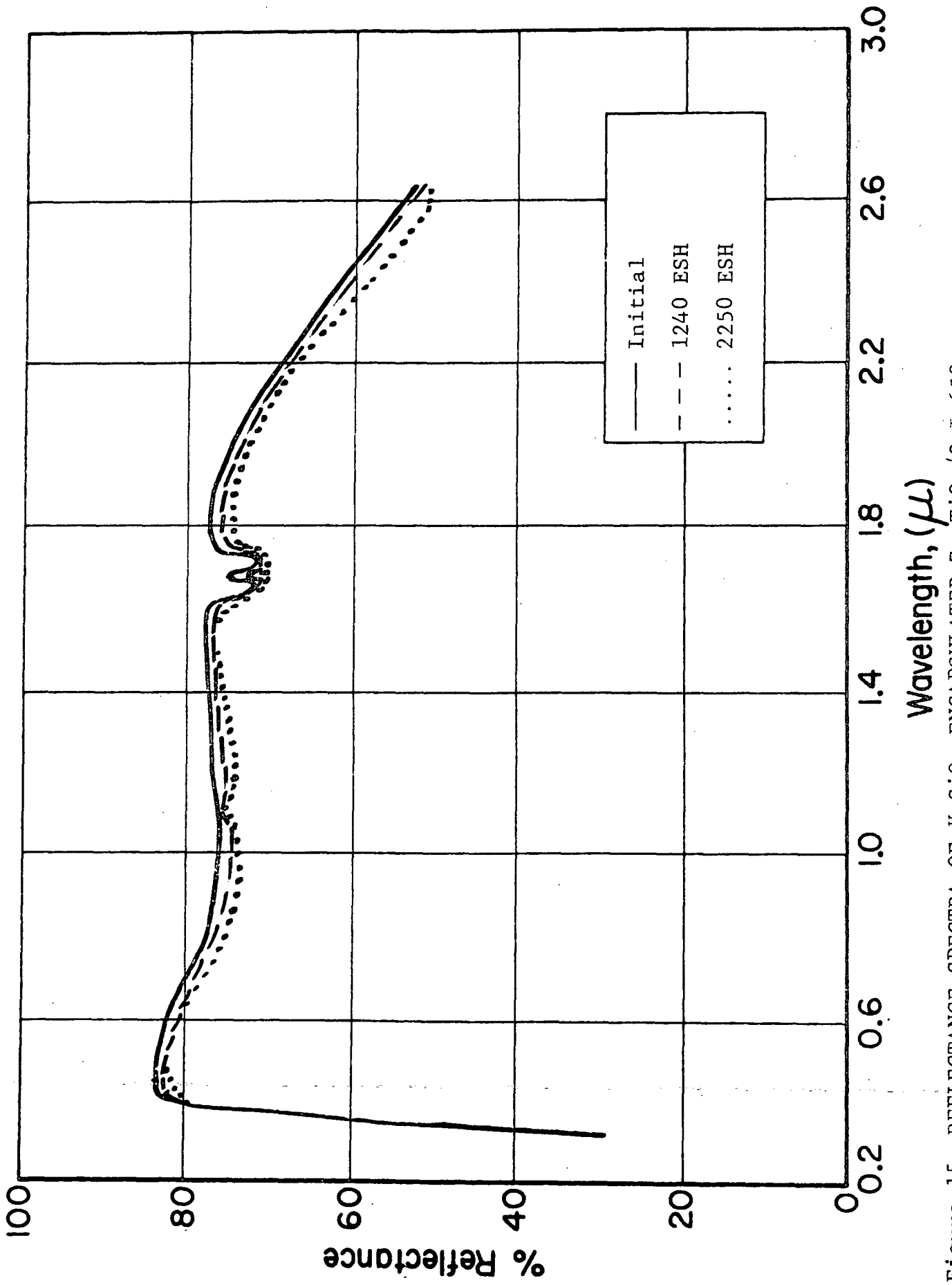


Figure 15 REFLECTANCE SPECTRA OF K_2SiO_3 -ENCAPSULATED $Zn_2TiO_4/O-I 650$

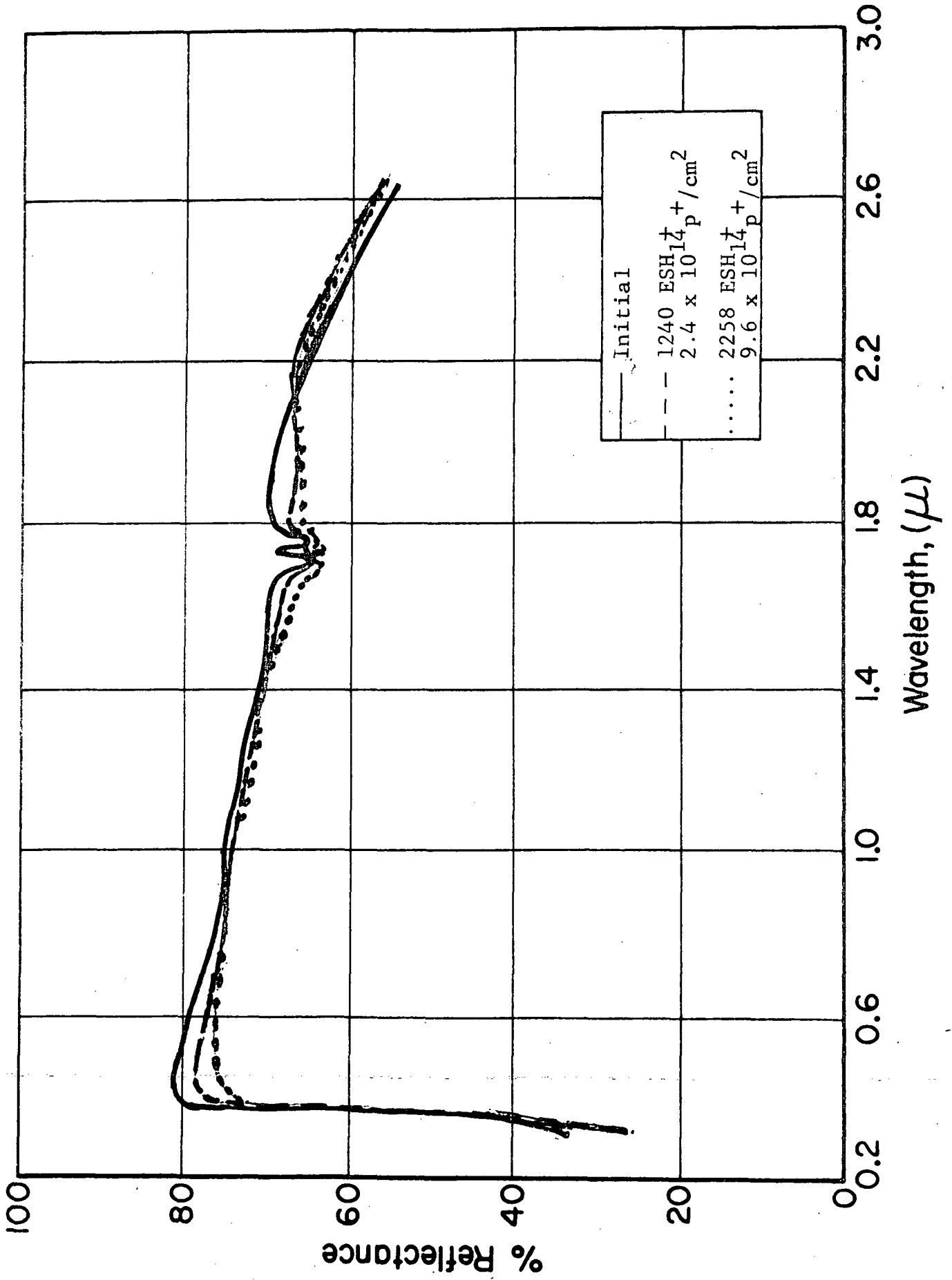


Figure 16 REFLECTANCE SPECTRA OF K₂SiO₃-ENCAPSULATED Zn₂TiO₄/O-I 650

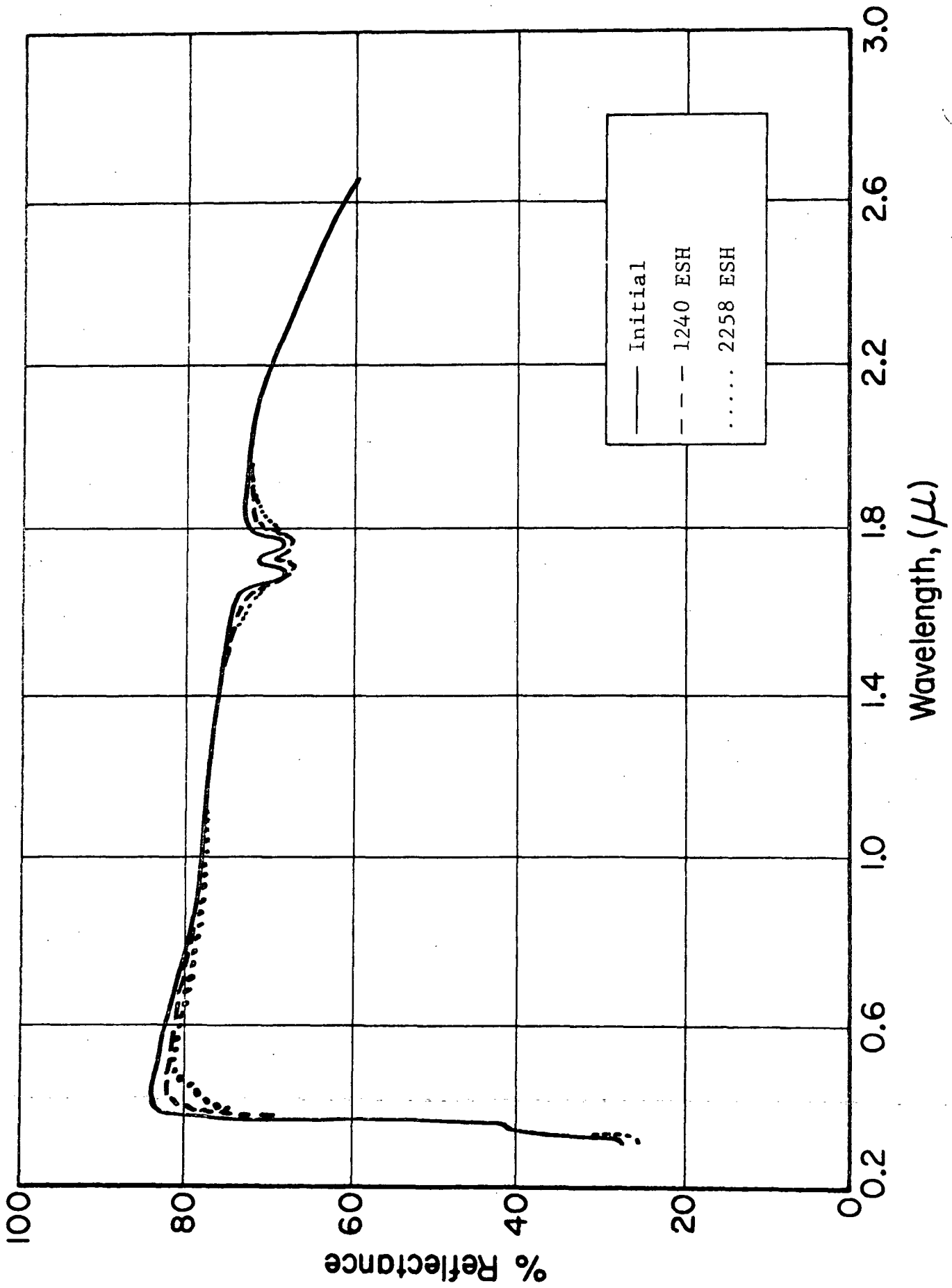


Figure 17 REFLECTANCE SPECTRA OF PLASMA ANNEALED, K_2SiF_6 -ENCAPSULATED $Zn_2TiO_4/0-1$ 650 MODIFIED

3.3.4 Analyses and Conclusions

The stability of Zn_2TiO_4 pigments which have been plasma-annealed compared to that of pigments not so treated has long been apparent. Plasma annealing, however, in certain cases evidently causes some permanent damage very similar to that it is intended to prevent. Although not considered very likely, the possibility exists that this damage was introduced in the grinding process after plasma annealing. In Figure 18 we compare the initial (unirradiated) spectral reflectance of $Zn_2TiO_4:K_2SiF_6$, with and without plasma annealing. The effect of the treatment is evident in the large induced absorption in the visible and near infrared regions of the spectrum centered at about 890 nm (the annealed pigment appeared "gray"). Stability of the plasma annealed pigment, however, was only slightly improved. In this case, the $\Delta\alpha_s$ attributable to plasma annealing alone is about 0.1. Table 4 summarizes the appropriate data from CREF-5 and CREF-6 for silicate paints of this pigment.

The performance of potassium silicate encapsulated Zn_2TiO_4 pigments is considerably better than that of any of the other encapsulated pigments. Table 5 compares the results obtained in CREF-5 with those in CREF-6 for the paints $Zn_2TiO_4:K_2SiO_3$ (Plasma)/O-I 650.

In Table 4, for comparable exposures, the results of Part 2 of the CREF-5 should be compared with those of Part 1 of CREF-6. The comparison is good, within experimental error. The stability of this latter paint system is very good. The largest part of the damage sustained by the paint after combined proton plus ultraviolet exposure is in the pigment, and most of that is due to ultraviolet radiation.

The data from CREF-5 and CREF-6 along with the results of many preceding tests make it very evident that, while plasma annealing does ordinarily improve pigment stability, it also in some cases has caused significant, and unacceptable, permanent increases in optical absorption - in one instance, greater than

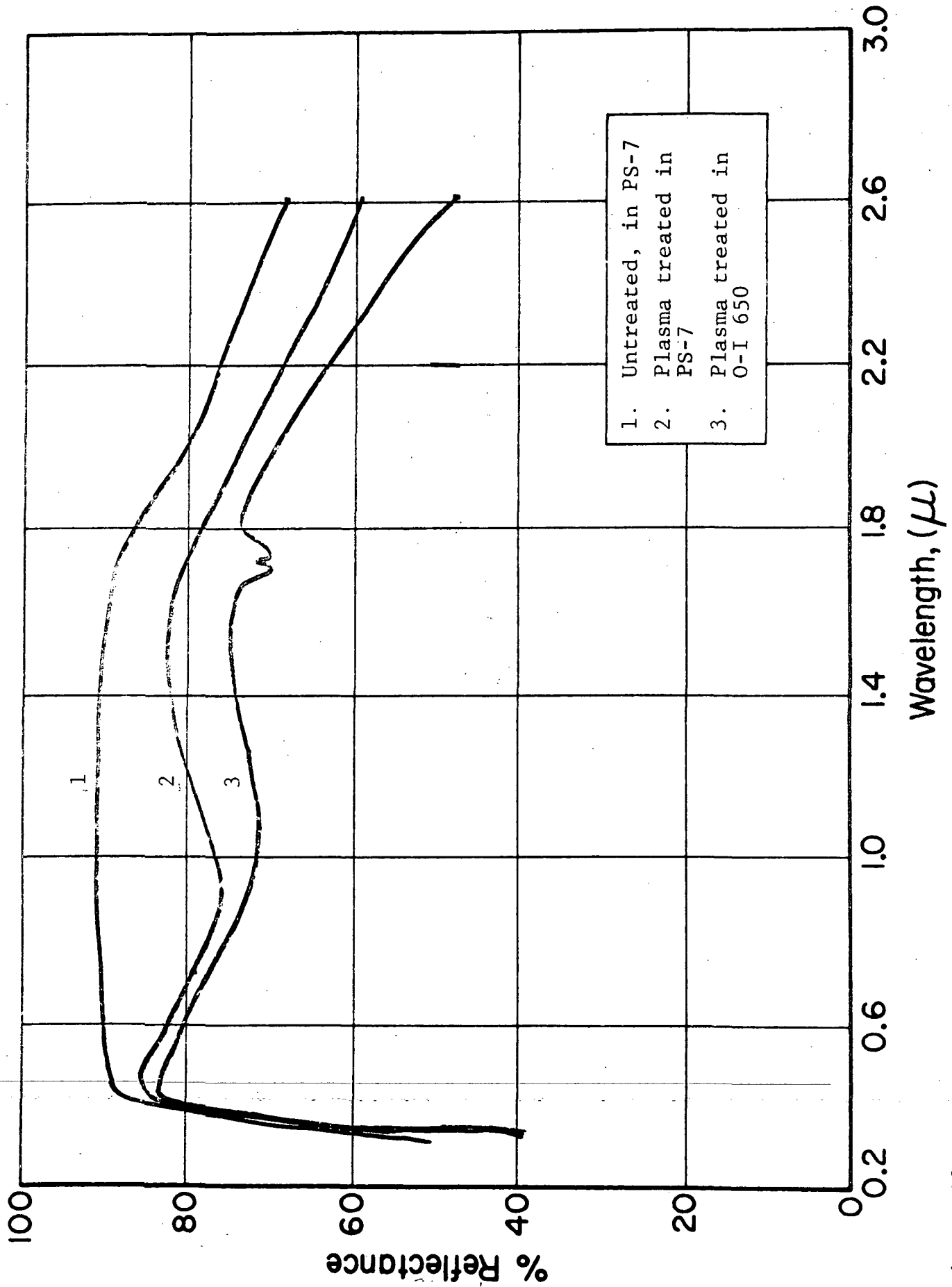


Figure 18 REFLECTANCE SPECTRA OF K_2SiF_6 -ENCAPSULATED Zn_2TiO_4 WITH AND WITHOUT PLASMA ANNEALING

Table 4

COMBINED IRRADIATION EFFECTS IN $\text{Zn}_2\text{TiO}_4:\text{K}_2\text{SiF}_6/\text{PS-7}$

<u>Exposure</u>	α_s Values		
	<u>Initial</u>	<u>Part I</u>	<u>Part 2</u>
<u>C-068 (CREF-5)</u> (Not plasma annealed)			
Protons only	0.158	0.204	--
Protons + ultra-violet	0.171	--	0.227
Ultraviolet only	0.179	--	0.204
<u>SRI-2 (CREF-6)</u> (Plasma annealed)			
Ultraviolet only	0.251	0.281	0.286

Table 5

COMBINED IRRADIATION EFFECTS IN $\text{Zn}_2\text{TiO}_4:\text{K}_2\text{SiO}_3$ (Plasma)/O-I 650

<u>Exposure</u>	α_s Values				
	<u>Initial</u>	$\Delta\alpha_s^*$	<u>Part 1</u>	$\Delta\alpha_s^*$	<u>Part 2</u>
<u>C-070 (CREF-5)</u>					
Protons only	0.194	(0.002)	0.196		
Protons + ultra-violet	0.223			0.013	0.236
Ultraviolet only	0.286			0.018	0.304
<u>C-169 (CREF-6)</u>					
Protons + ultra-violet	0.290	(0.013)	0.303	(0.025)	0.315
Ultraviolet only	0.243	(0.009)	0.252	(0.017)	0.260

* $\Delta\alpha_s$ values determined with respect to initial value.

the $\Delta\alpha_s$ caused environmentally in a pigment not plasma annealed. Some pigments, therefore, are benefitted more from the plasma heat treatment than others. In theory, however, the plasma heating conditions can be optimized to produce stable pigments without otherwise affecting their optical properties. An analysis of all the available data suggest that, to be successful, the plasma annealing process must affect the pigment surface - and only the pigment surface; otherwise, internal high temperatures cause significant permanent optical damage. The nature of the encapsulant consequently takes on a more important role than previously ascribed to it. Overall optical stability would thus relate to its interaction with the pigment and how this is affected by the plasma treatment. The facts that plasma heat treatment damages some encapsulated pigments more than it benefits them and that some encapsulants are nearly as effective as an ideal plasma heat treatment suggest that the "stable" surface treatment may be attainable chemically as well as by plasma annealing. We have not found the universal key yet in either approach, but for best results, currently, both are required.

3.4 Solar Simulator Monitoring

The intensity spectrum of extraterrestrial solar radiation has long been a difficult one to reproduce in the laboratory. In the field of spacecraft thermal control the question of what source to use as a solar simulator has never been adequately answered. Two significant facts to consider are that a practical source which exactly simulates the solar spectrum is not available, and the effects of a spectral mismatch are unknown.

The lack of an exact solar simulator for practical laboratory applications stems from many factors - not the least of which is ~~the aging effect or lack of spectral intensity stability - of most~~ "reasonable" simulators. As for a spectral mismatch, the question of what are its affects becomes highly complicated by the fact that the absorption spectrum of the tested materials becomes very important; different materials will absorb different amounts of

"damaging" radiation - in different spectral regions. Ultimately, then, the issue comes down to this: since exact simulators are unavailable, the use of "conservative" sources - those which over-simulate - seems to be indicated.

Whatever source is used, a means of defining equivalent exposures is a necessity. The definition universally employed for this purpose is that of the Equivalent Sun-Hours (ESH) - the total ultraviolet energy ($\lambda < 4000 \text{ \AA}$) incident on a plane surface outside the earth's atmosphere at a distance of one astronomical unit (A.U.) from the sun. Accordingly, when we use a solar simulator we must know how much energy it radiates in the region below 4000 \AA . The spectral intensity distribution for simulation purposes is, of course, the central question; in terms of the ESH definition only the integrated energy ($0 < \lambda < 4000 \text{ \AA}$) is important. The spectral intensity distribution, however, must be known, in order to be assured that the source is radiating ultraviolet energy in the 1800-2000 \AA region, where most dielectric materials of interest to us absorb. This discussion is intended to serve only as a very brief background to the subsequent discussions of our ultraviolet monitoring studies.

The work reported here was accomplished in order to determine the spectral intensity distributions of IITRI's solar simulators and to obtain their performance-vs-time and lifetime characteristics. This information will be valuable not only in calculating ESH data but in selecting appropriate, sensitive wavelengths to monitor during irradiation.

3.4.1 The AH-6 Solar Simulation System

For routine irradiations we utilize a PEK Labs 1000 watt, water cooled, high pressure, mercury-argon AH-6 lamp. The major reasons for using the AH-6 system are mainly that this source is very rich in ultraviolet radiation and that its ultraviolet intensity spectrum matches "reasonably well" that of the extra-terrestrial solar electromagnetic radiation. Approximately

one-third of the radiant energy of this source lies in the ultraviolet portion of the spectrum.

We recognize the shortcomings of this source in terms of achieving true solar simulation but, as a source for screening materials or comparing their performance, it is one of the best. The high fraction of ultraviolet radiation has several very practical advantages. Acceleration factors as high as ten (10) are possible without the risk of significant sample heating. By way of comparison the mercury-xenon lamp operates at four (4) equivalent suns with an input of 5000 watts, while 1.5 equivalents is an upper limit for the 5000W xenon system. The choice between any of these is not obvious, when simulation requirements, costs, spectral mismatch effects, aging effects, etc. are considered.

The major problem associated with the use of the AH-6 mercury-argon lamp is that they exhibit erratic lifetimes and instability of spectral distribution as a function of age and number of re-starts. IITRI personnel in the early 1960's (Ref. 5) studied the AH-6 system using a Jarrel-Ash spectrometer; they reported definite trends in the bulb's intensity spectra. Shifting of major peaks or complete disappearance of these peaks were noticed, and also that each bulb's aging characteristics are almost unique. The intensity spectra and aging trends were similar but exact reproducibility from bulb to bulb was non-existent. This being the case the development of some spectra-measuring device to check these bulbs was necessary if not mandatory.

3.4.2 Experimental Equipment

The purpose of the experimental equipment described here is to obtain spectral intensity measurements of the radiant output of our solar simulation sources. Experimental measurements were made through the use of a monochromator, a light chopper, a sodium salicylate phosphor, a silicon diode fluorescence detector, and a lock-in amplifier (phase locked to the chopper). A schematic diagram of the arrangement is shown in Figure 19.

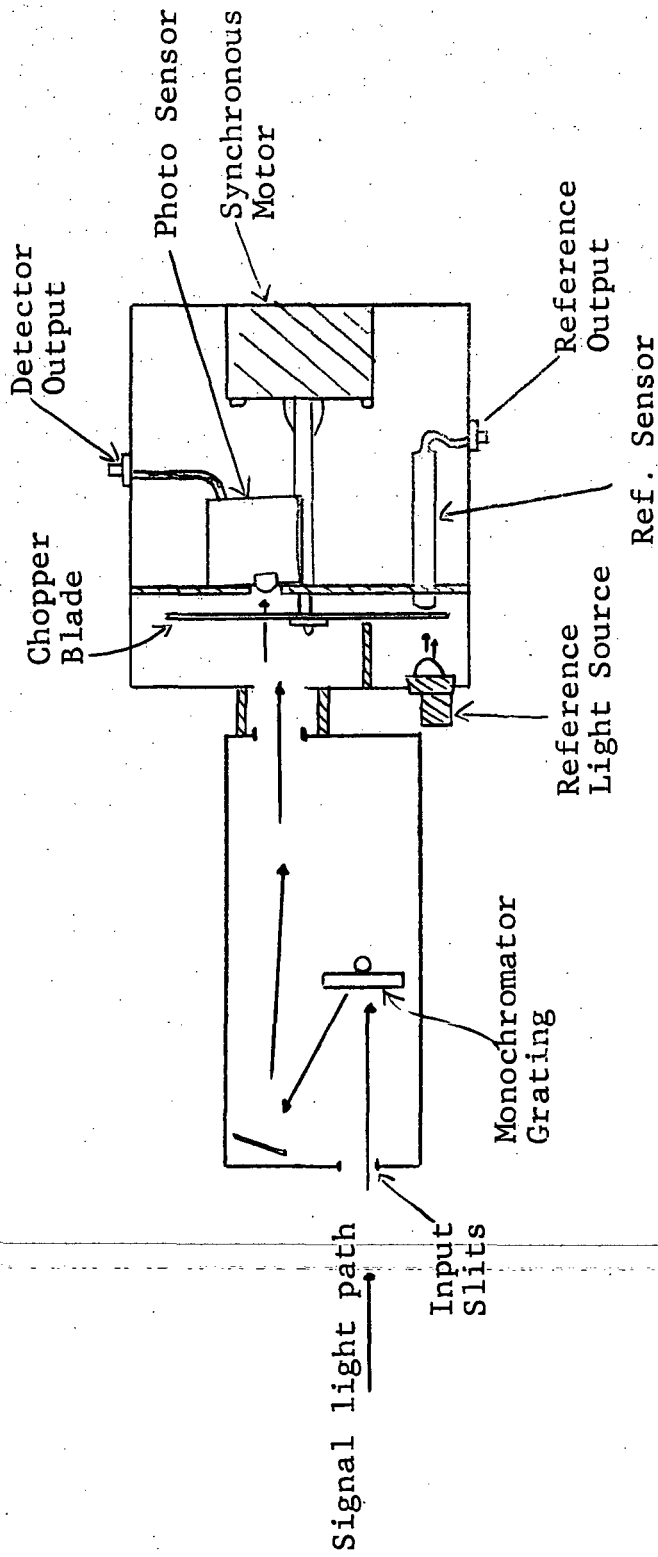


Figure 19 BLOCK DIAGRAM OF SPECTROMETER/DETECTOR ASSEMBLY

Light energy from the simulator enters the spectrometer through the entrance slits of a Bausch & Lomb Model 33-86-01 monochromator. The dispersed (monochromatic) light energy is then chopped by a 1000 cps constant speed chopper assembly. The chopped beam then falls on the salicylate detector, the fluorescence from which is directly proportional to the incident ultraviolet radiation intensity. The salicylate fluorescence, which peaks at $\lambda = 410$ nm, is detected by the silicon photodiode. The detector signal is amplified and displayed either on an oscilloscope or on a recorder. The salicylate detector is prepared by spraying a 10 mg/cm^2 film of sodium salicylate from a methanol solution onto a clean substrate (usually a pyrex microscope slide). This film absorbs ultraviolet energy and transmits energy in the visible. The spectral response curves for the photodiode and the salicylate detector, and the intensity spectrum of the salicylate fluorescence are given in Figures 20, 21 and 22. These curves are taken from EG&G, the diode manufacturer, from Ref. 5, and from Ref. 6, respectively.

A reference beam of light enters the sensing housing but is isolated from the sample signal so no mixing can occur. This light originates from a small D.C. light source located directly in front of the chopper blade assembly where it is also chopped to 1000 cps, providing the lock-in frequency signal to the amplifier.

The outputs of both sensors, the sample signal and the reference signal, are then individually amplified by Packard Model 466A AC-Amplifiers whose impedances are matched to that of the Princeton Applied Research Lock-In Voltmeter/Amplifier (Model JB-5).

The Princeton Amplified Research (Lock-In Voltmeter), referred to as the PAR, then measures the intensity of the sample signal in voltage units. The PAR, being a lock-in voltmeter, locks in on the chopper frequency, in our case 1000 cps. Once locked in, it strongly discriminates against all other frequencies. Intensity

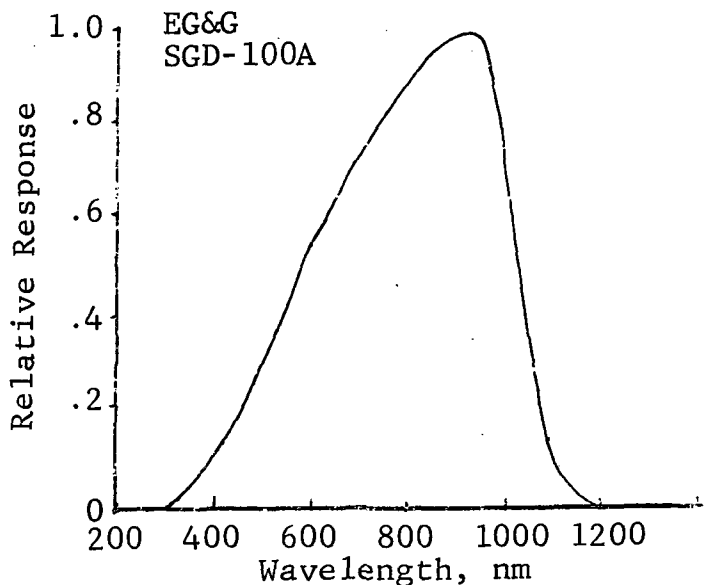


Figure 20 SPECTRAL RESPONSIVITY CURVE (EG&G DATA)

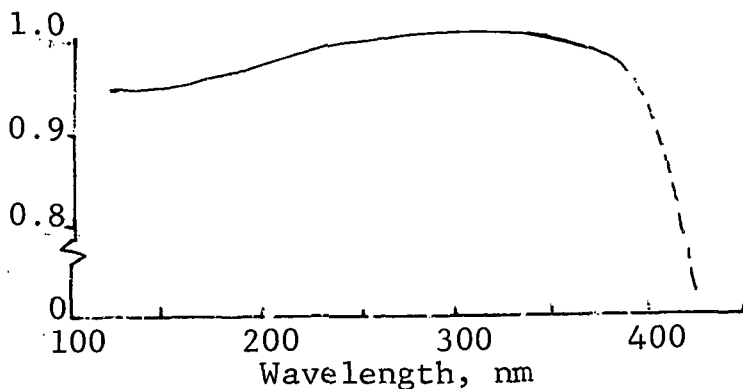


Figure 21 QUANTUM EFFICIENCY OF SODIUM SALICYLATE (Ref. 6, 7)

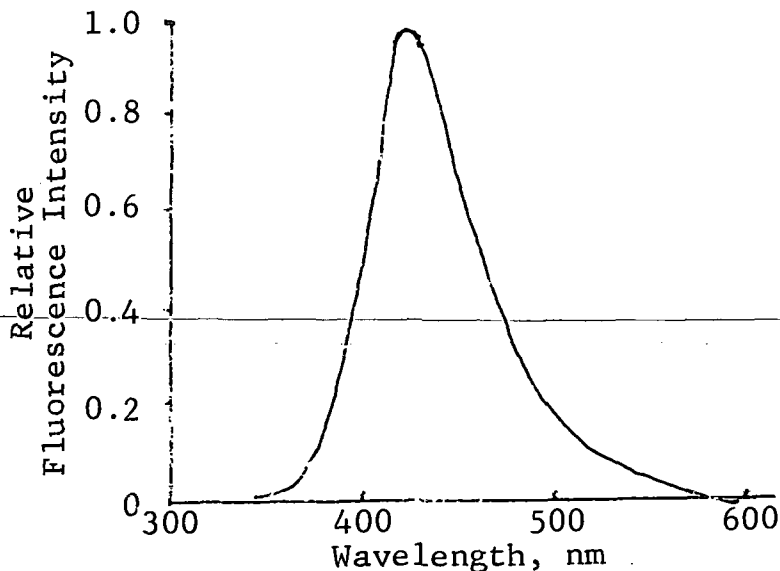


Figure 22 SPECTRAL FLUORESCENCE INTENSITY OF SODIUM SALICYLATE (Ref. 7)

measurements giving rise to signals of the order of 10^{-10} volts are not uncommon for the PAR and its use in conjunction with the photodiode gives highly satisfactory sensitivity.

In Figures 23 and 24 the electrical schematic diagrams of both photodiode assemblies are presented. Both the sample and reference photo-sensors incorporate simple electrical circuitry for operation. The photodiode in the sample circuitry is EG&G Model SGD-100A. This particular diode is accurately calibrated and stable, but is very sensitive to voltage polarity; it must operate in the range of -20 to -90 VDC. The photodiode used in the reference sensor, not being required for accuracy, is a simple duodiode capable of operating on any voltage in the range of ± 1 to 125 VDC (depending upon level of output desired).

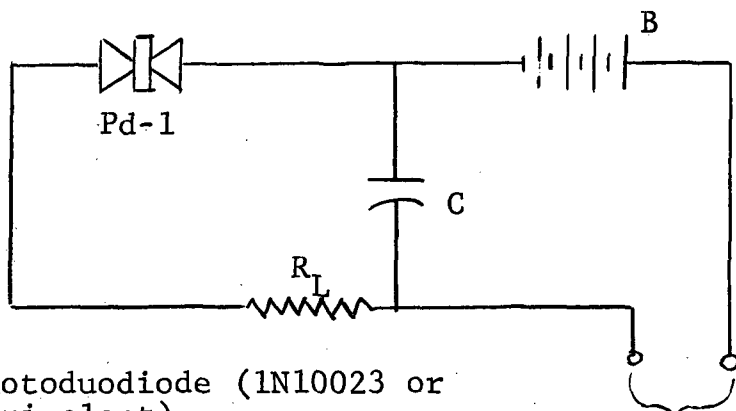
Photographs of the chopper-detector assembly, the spectrometer and the PAR, and of the overall experimental set-up are shown in Figures 25, 26 and 27 respectively.

3.4.3 Experimental Results

In this section we present intensity spectra of IITRI's currently used solar ultraviolet simulators. In Figures 28 and 29 we have reproduced the spectra published by manufacturers of the lamps - PEK, Inc., and Hanovia Div. of Canrad Precision Ind., Inc. With the equipment previously described, scans were taken of the radiant output of a new AH-6 lamp at the start of a simulation test, again after 72 hrs of operation, and finally at the completion of a test of approximately 166 real time hrs.

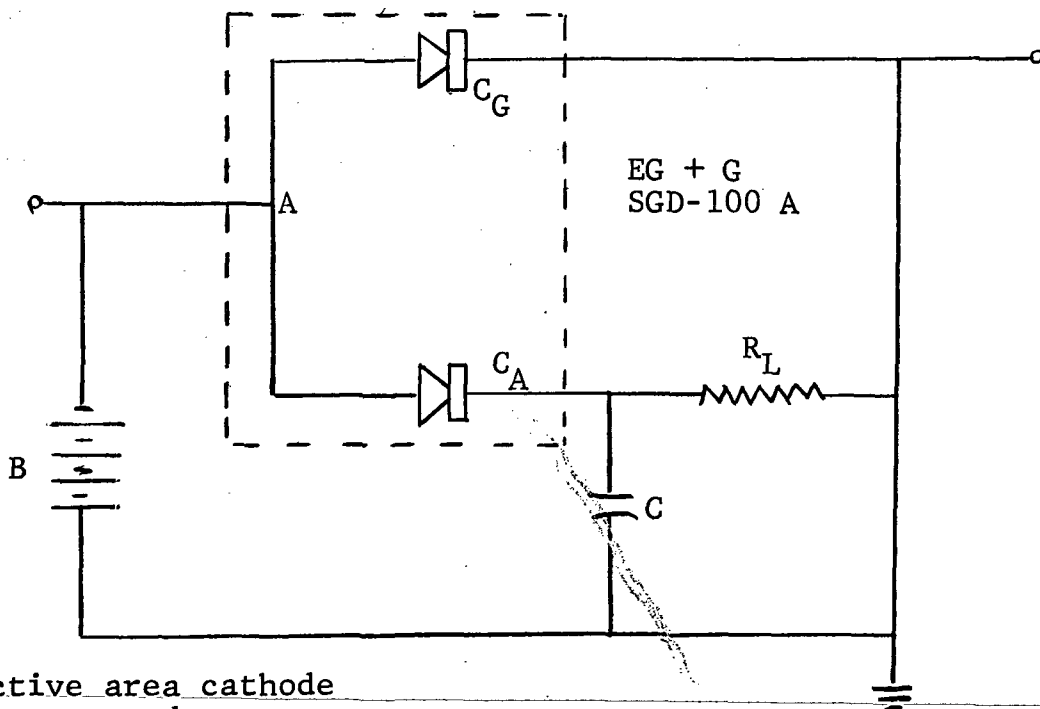
The above three spectra are shown in Figures 30, 31 and 32, and are superimposed in Figure 33. Some intensity peaks have disappeared (e.g. in the 3500 Å region), while others seemed to have shifted in wavelength (e.g., near the 3200 Å peaks).

The data presented are only semi-quantitative, because we wished only to establish relative values and trends, e.g., the relative "aging" of the irradiation sources. Accurate measurements will be possible when calibration of the overall detector



- Pd-1: Photodiode (1N10023 or equivalent)
 R_L : Load resistor (~ 1 meg-ohm)
 C : Filter capacitor (.01 μ fd.)
 B : DC voltage source (0-125V)

Figure 23 SCHEMATIC OF REFERENCE PHOTODIODE CIRCUITRY



- C : Active area cathode
 A : Common anode
 C_G : Grounding cathode
 R_L : Load resistor (~ 1 meg ohm)
 C : Filter capacitor (.01 μ fd)
 B : DC power source (20-90V)

Figure 24 SCHEMATIC OF PHOTODIODE SENSOR CIRCUITRY

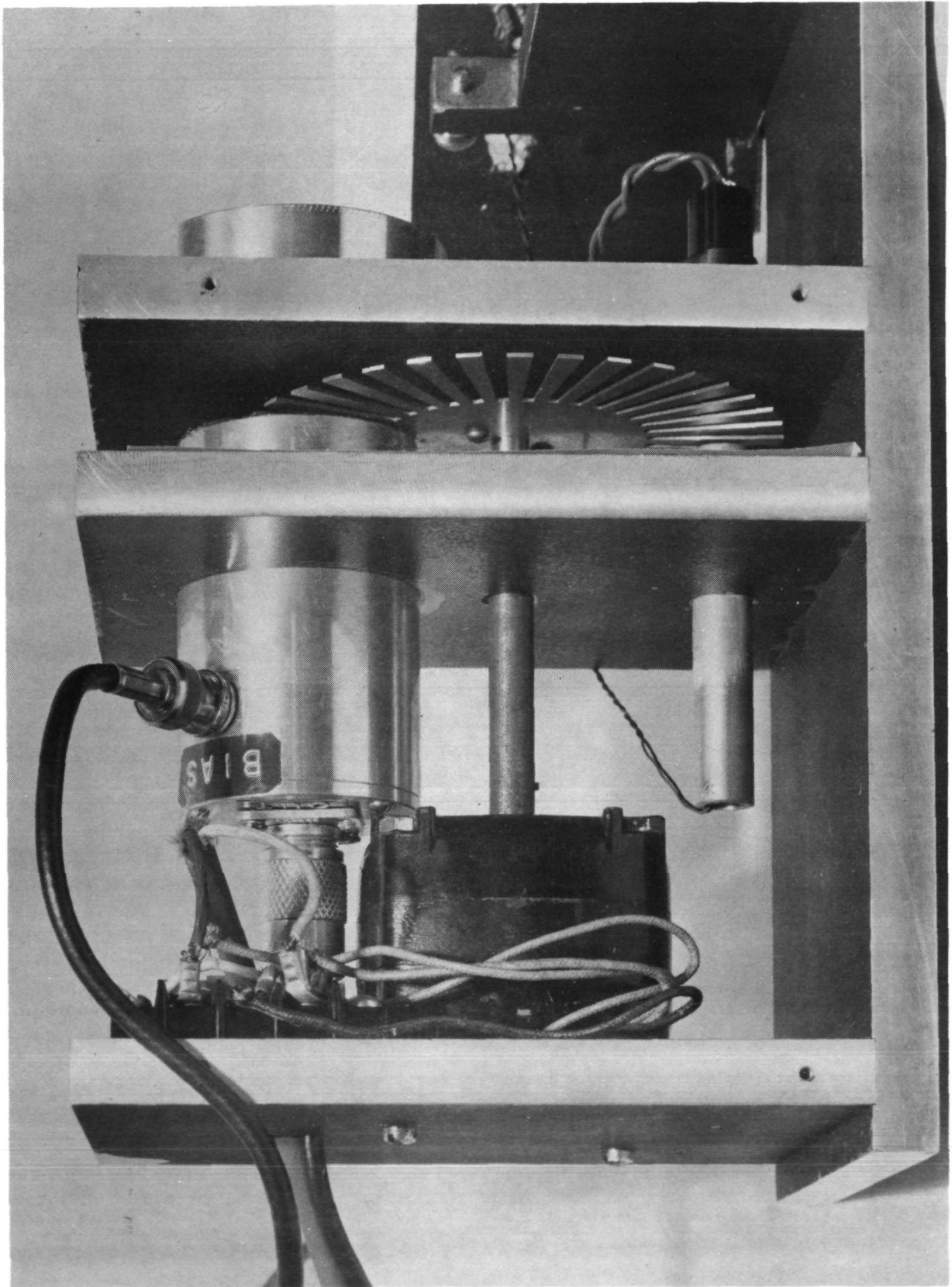


Figure 25 CHOPPER-DETECTOR ASSEMBLY

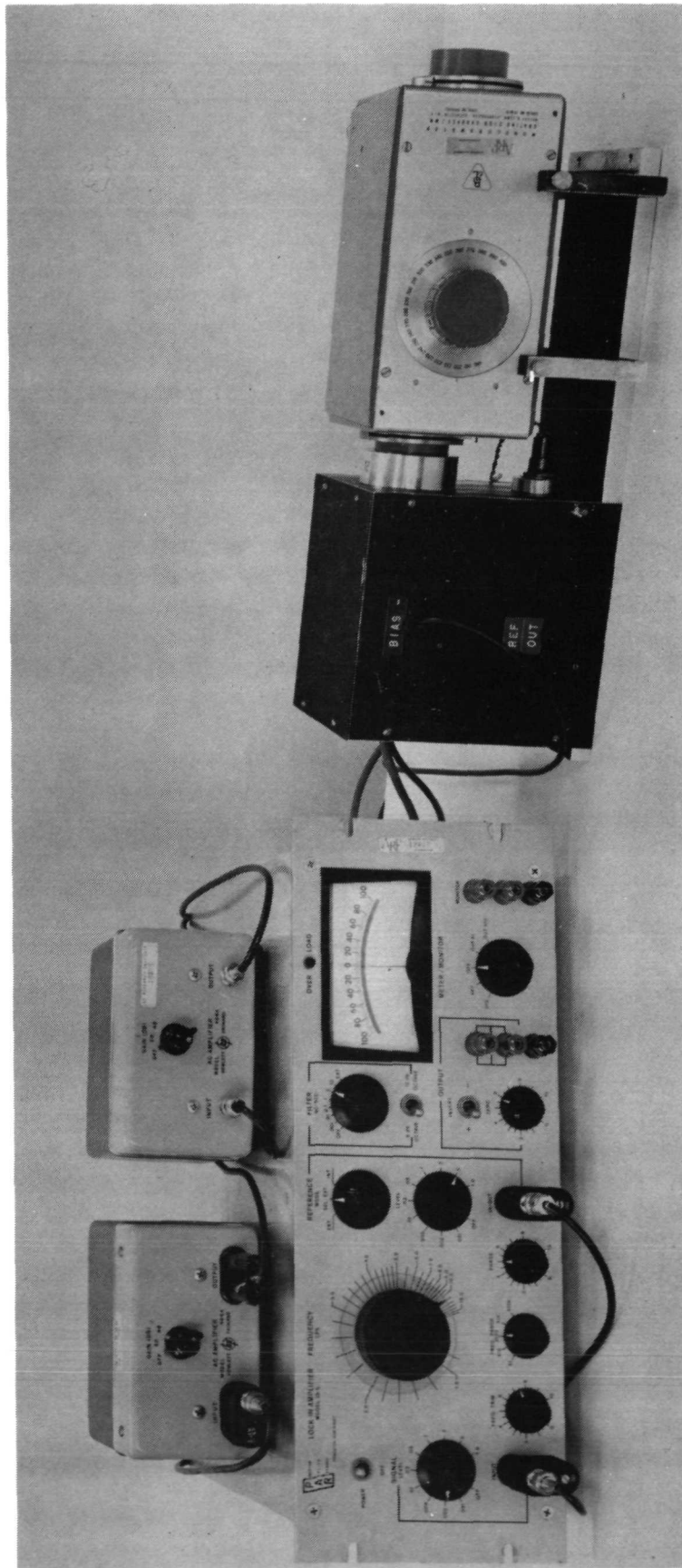


Figure 26 SPECTROMETER AND THE PAR

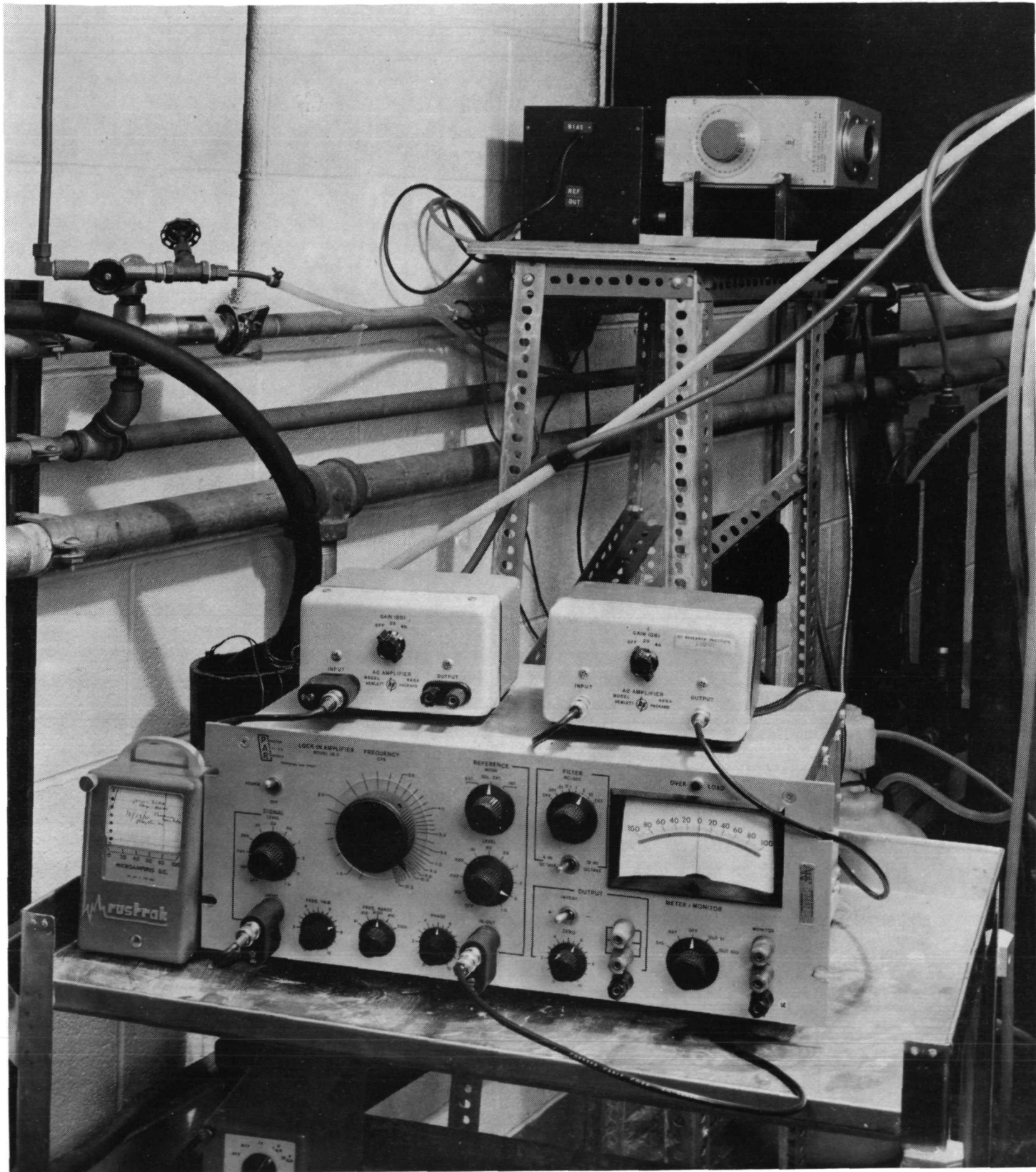


Figure 27 EXPERIMENTAL SET-UP

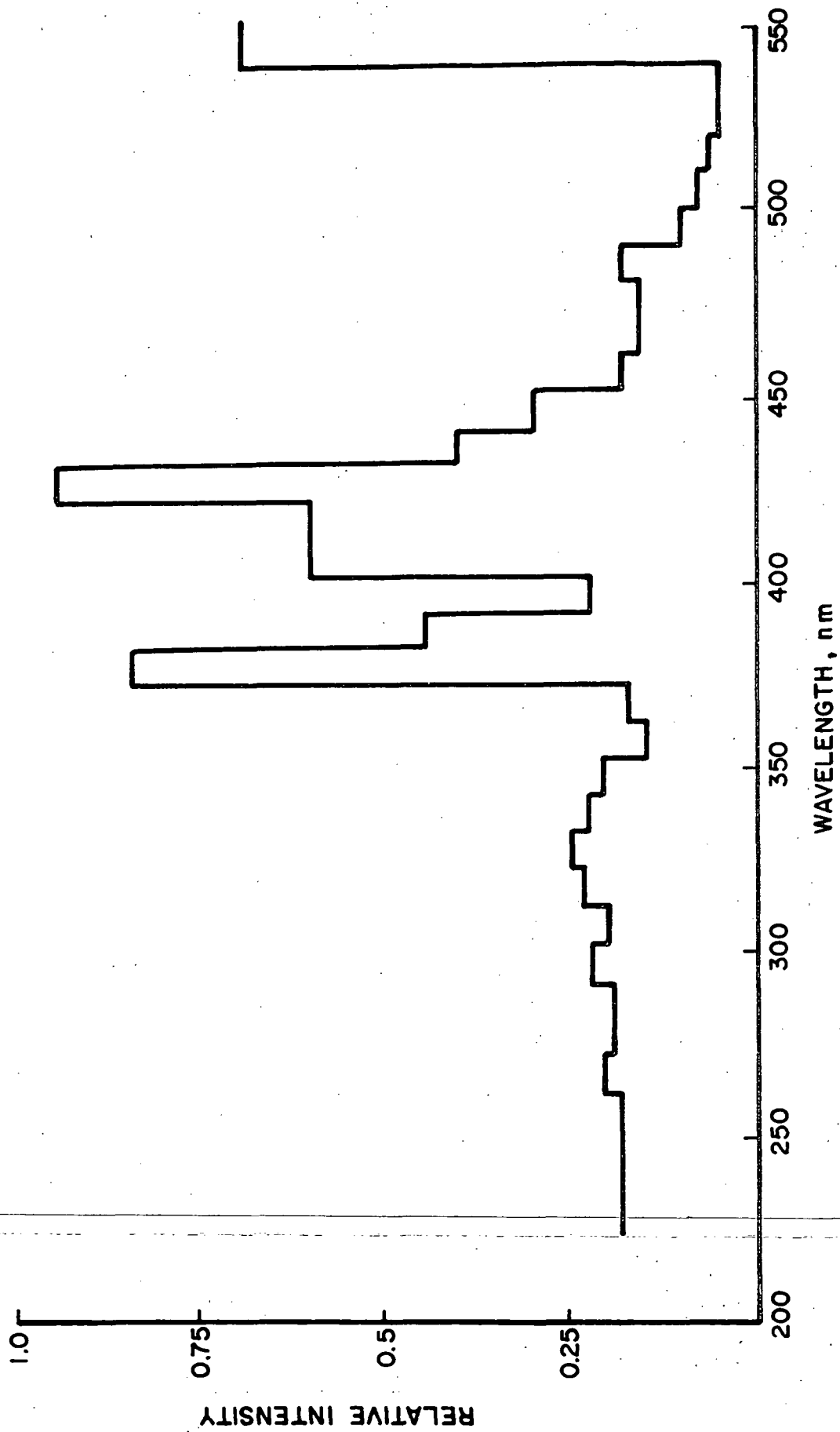


Figure 28 AH-6 INTENSITY SPECTRUM-MANUFACTURER'S DATA

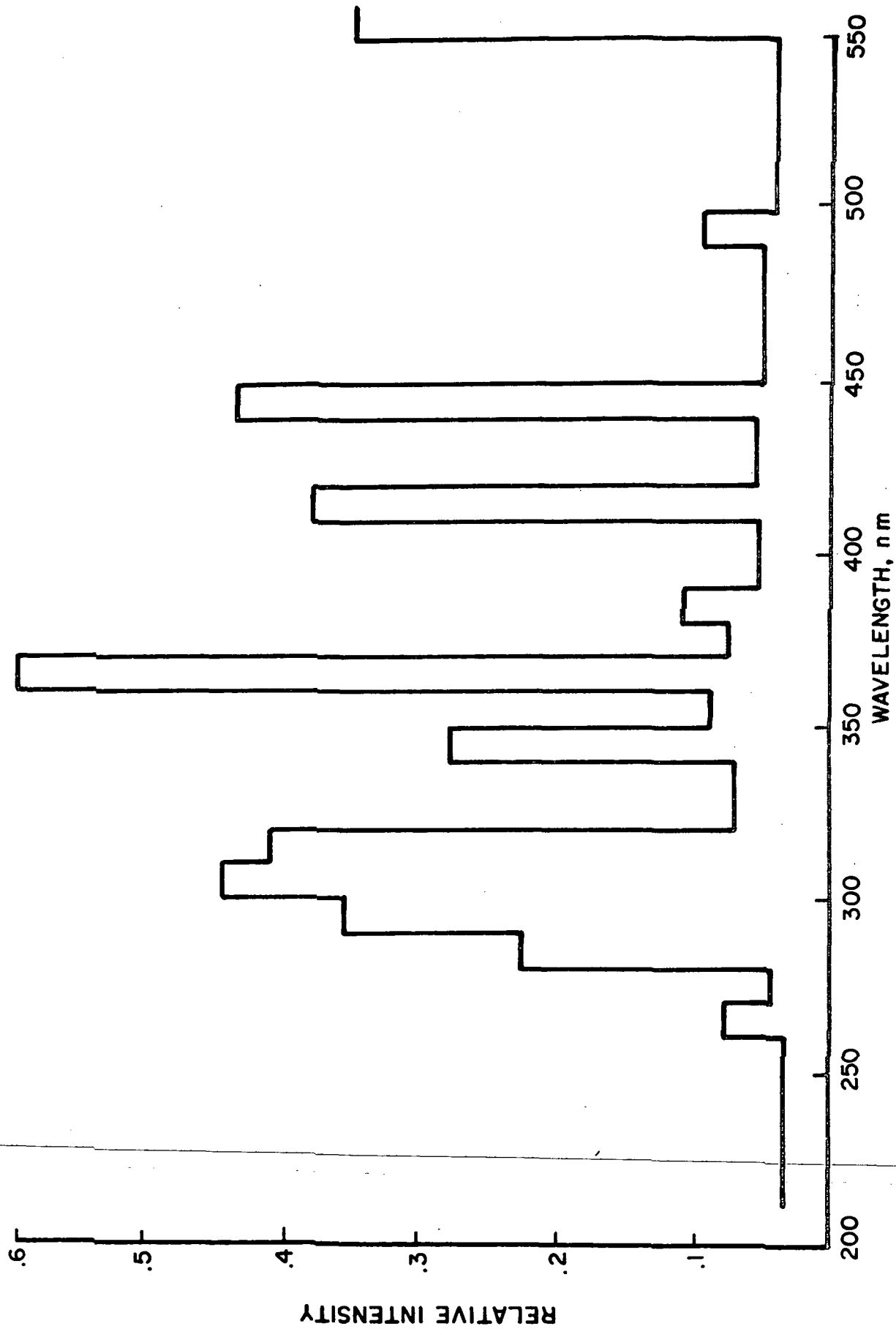


Figure 29 SPECTRAL RADIANCE OF NEW HANOVIA 5000W MERCURY-XENON LAMP-MANUFACTURER'S DATA

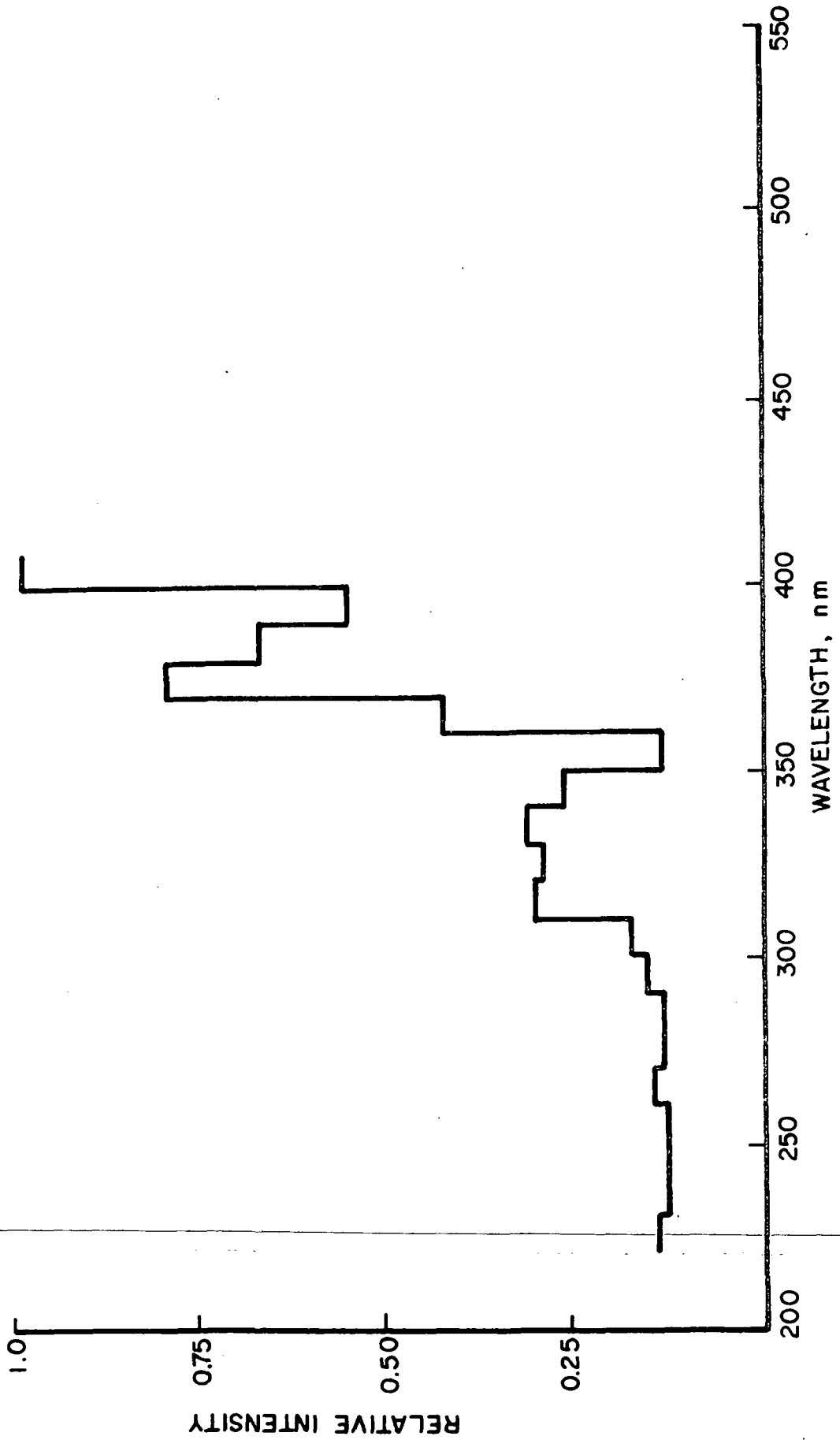


Figure 30 AH-6 INTENSITY SPECTRUM - 0 HRS (NEW)

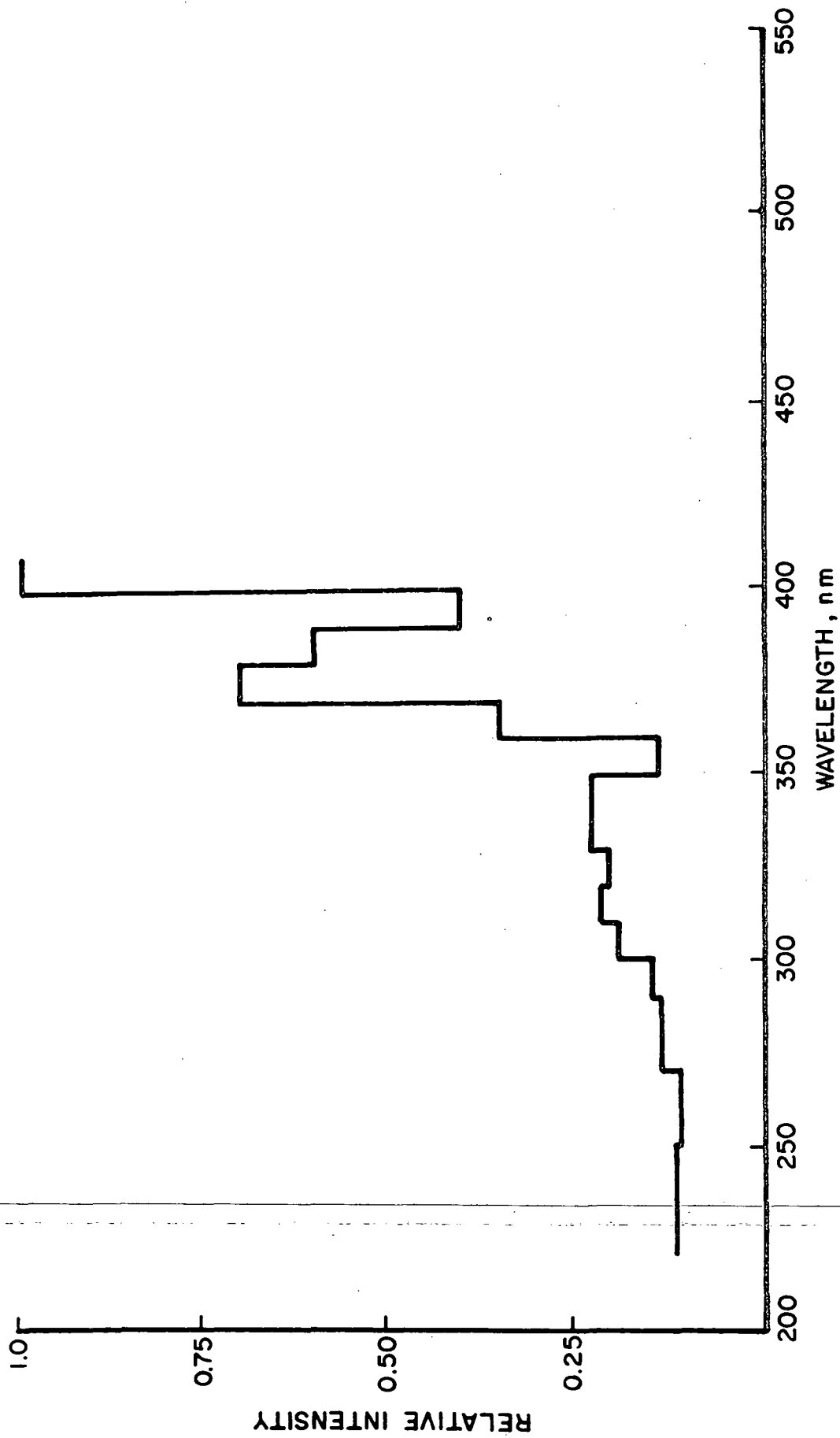


Figure 31 AH-6 INTENSITY SPECTRUM - 72 HRS.

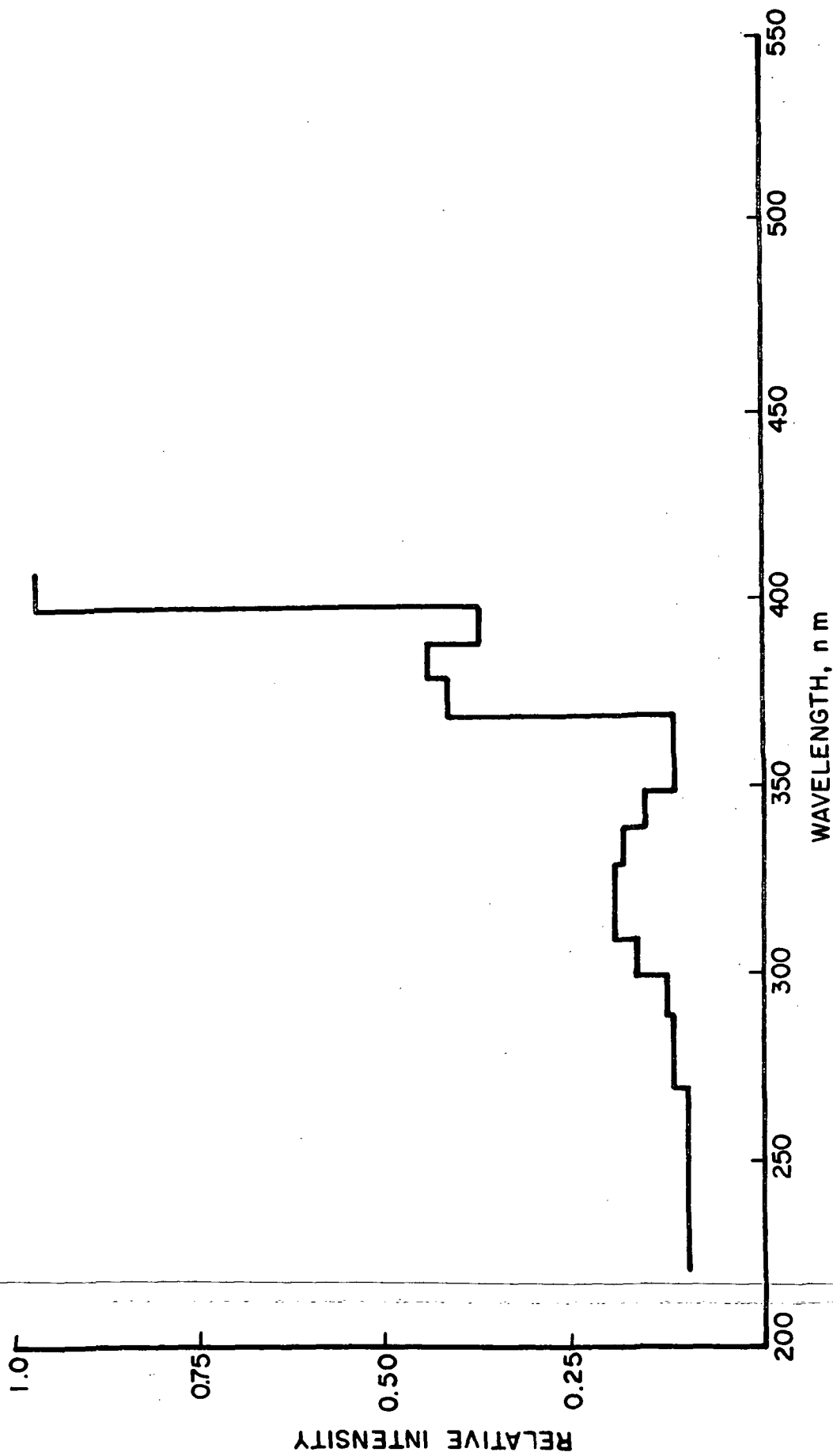


Figure 32 AH-6 INTENSITY SPECTRUM - 167 HRS.

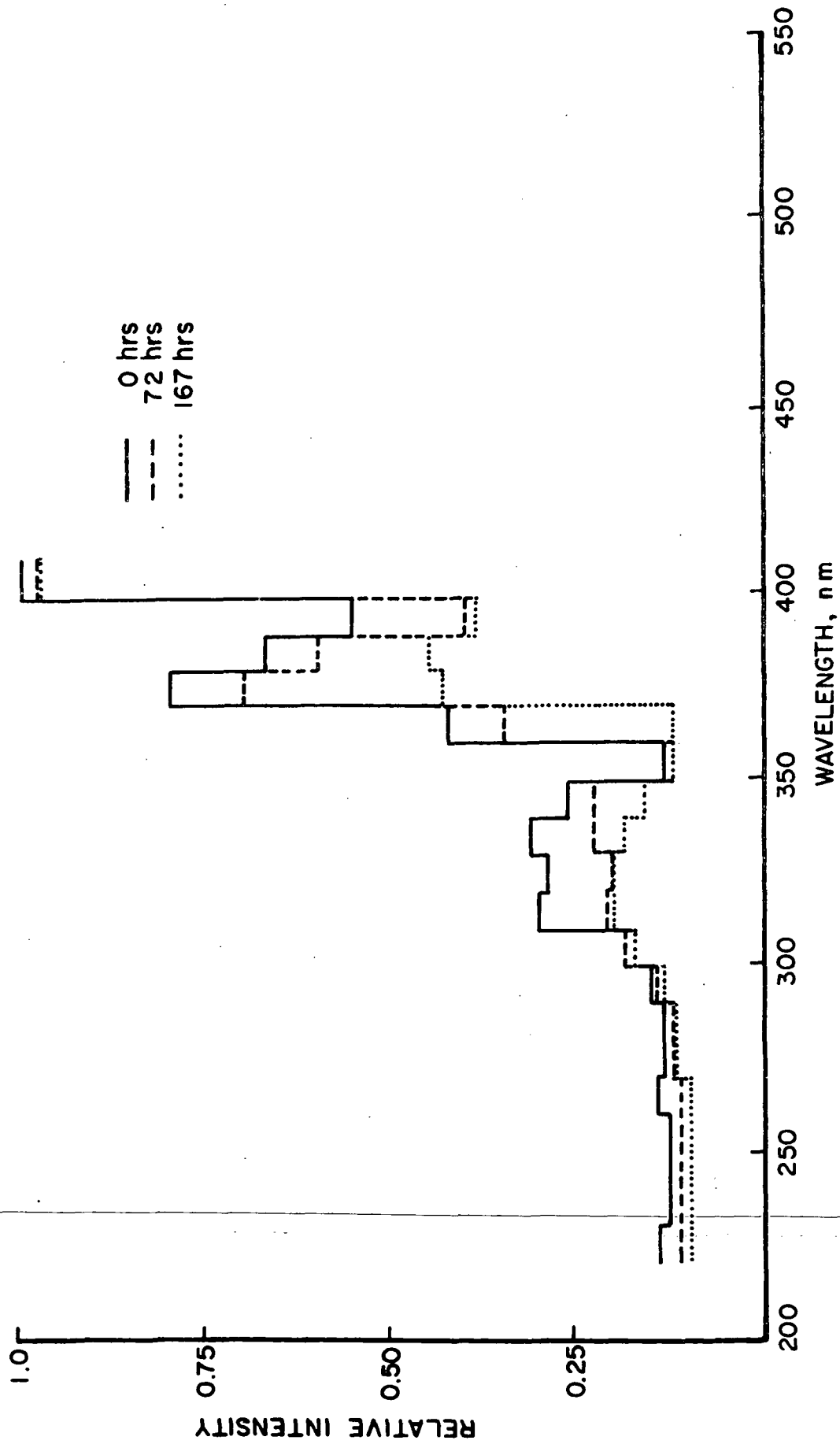


Figure 33 AH-6 INTENSITY SPECTRA - COMPOSITE

system (frequency response, etc.) and of the monochromator (effective band widths, absorption losses, etc.) are accomplished. For comparative purposes, however, these data are highly useful and be used in evaluating the performance of individual bulbs. The data clearly indicate for example, which wavelengths are most affected by aging.

Currently, an Hanovia 5000 watt Mercury-Xenon arc lamp assembly is used in the CREF and has been operating successfully for the last six (6) months. The operating life of this assembly, which is of the order of 750-1000 real time hours, is superior to that of the AH-6, and this lamp apparently does not suffer significant operating changes with time or number of restarts.

Figure 34 shows a scan of the Hanovia lamp from 200 nm to 600 nm or mainly the near ultraviolet region which is important in the solar simulation spectrum. Superimposed upon the lower spectrum is one of the same lamp operating at a higher voltage (50 VAC). The higher voltage increases the ultraviolet output mainly by initiating a better vaporization of the Mercury in the bulb; however, operation at higher power levels tends to shorten the useful life of this source.

Comparison of these two spectra reveals less than a 10% decrease in energy as a result of reducing the operating voltage from 50 to 30 VAC. The slight reduction in ultraviolet radiant power is more than offset by the added operating life. At full power (~50-55 VAC) the useful life is approximately 500 hrs; at the lower power setting (30 VAC), useful lifetimes of as much as 1000 hrs are common.

The effect of re-starting (or cycling) an AH-6 lamp assembly has also been studied. The radiant output is shown with a time axis in Figure 35 for a new lamp immediately after starting it, after being turned-off, and after having been restarted several times (after a short cooling period in between). Changes in total energy output definitely occurred. The total energy was measured by a calibrated thermopile.

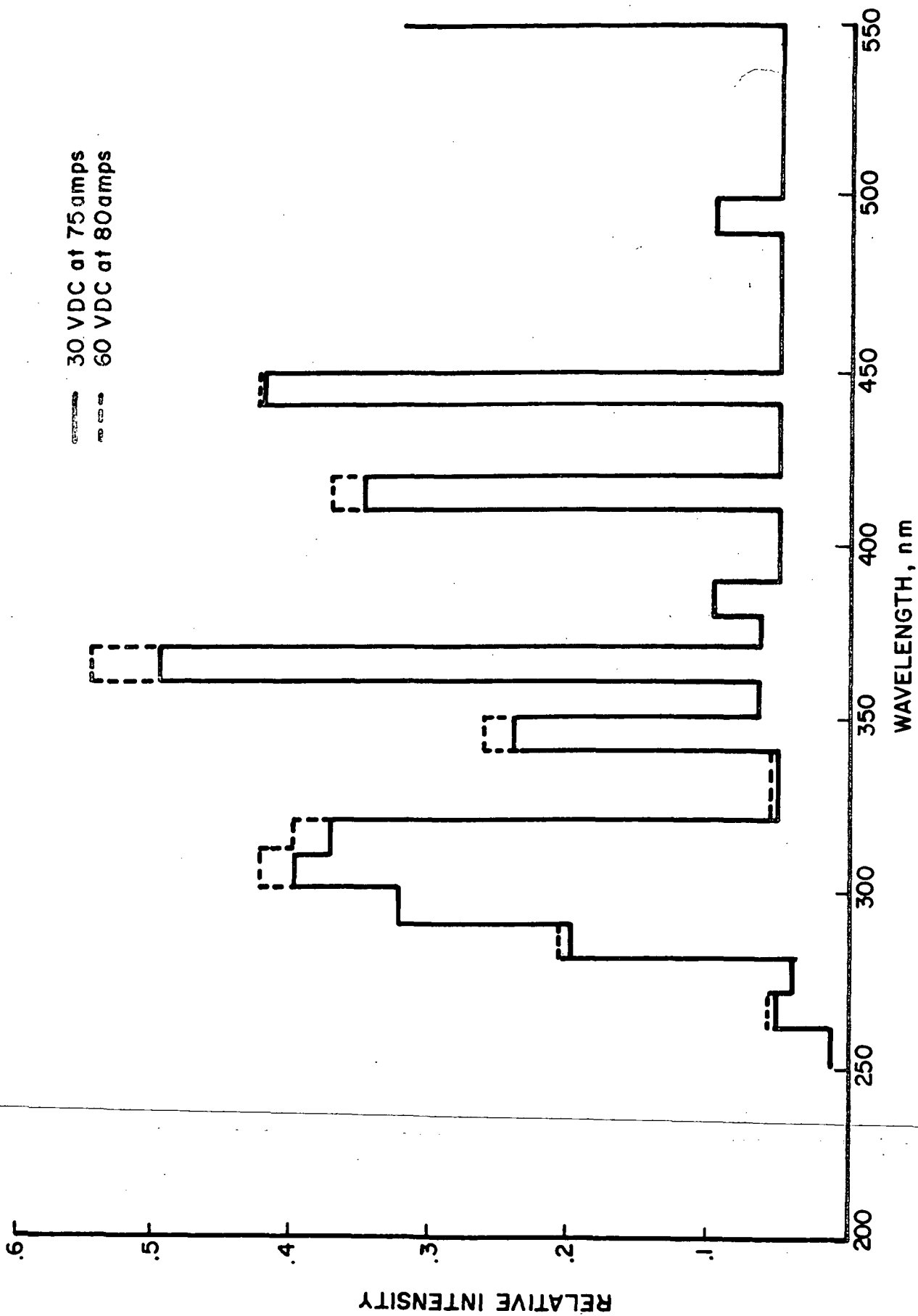


Figure 34 SPECTRAL RADIANCE OF HANOVIA 5000 WATT MERCURY-XENON LAMP

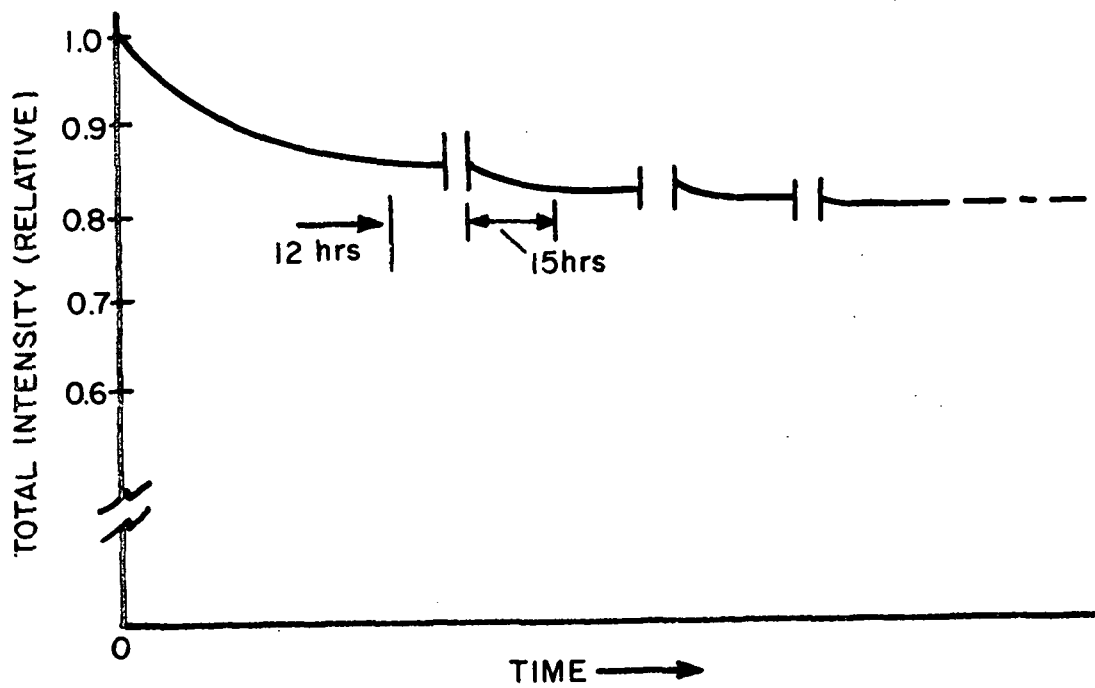


Figure 35 RESTART EFFECT ON AH-6 RADIANT OUTPUT

After starting the lamp its output reached equilibrium after approximately 12-15 hrs. The lamp was then turned off and allowed to cool. After cooling it was restarted and the output again recorded. This procedure was repeated several times.

The second restart required less time to reach equilibrium than the first. A loss of 2-4% was noted on the second, third and subsequent restarts. The first restart, therefore, seems to be the most significant with respect to its effect on radiant output in that it accounts for a total loss of approximately 10-15%. At least in the case of AH-6 lamps, restarts as well as longevity of the lamps clearly are important considerations in terms of solar simulation.

3.4.4 Future Work

An accurate calibration of the overall system will be initiated. This is possibly the most difficult problem to be undertaken, because it involves using either (1) a calibrated source (in the sense that its energy output in one or more specific wavelength regions is well known; or (2) a calibrated detector. Either method is somewhat tedious; but, once accomplished, the monitor system will be completely characterized and useful for quantitative spectral intensity measurements.

We will continue to obtain spectral intensity measurements of the AH-6 lamps and of the Mercury-Xenon sources in order to develop better statistics on their respective operating characteristics. The present plan calls for an initial, an intermediate and a final scan on each Mercury-Xenon lamp. AH-6 lamps will require a schedule which is commensurate with the operating schedule relative to the number of re-starts.

4. GENERAL COATINGS INVESTIGATIONS

4.1 Introductory Remarks

Thermal control surfaces for spacecraft are very likely to be only as reliable as the protective means taken to assure and maintain their cleanliness while in storage, because all surfaces and surface coatings, even the most stable, are susceptible to contamination. During the period after application of a paint to a spacecraft surface up to the time of vehicle launch, external surfaces will be exposed to numerous environments, human handling and storage to name but two. The types of contamination are legion; the effects, however, are of two general kinds. The first is due to the fact that contamination contributes optical absorption initially and as it degrades, thus increasing α_s . The second, and by far the more important, effect is the potential acceleration of ultraviolet damage in the paint. The effect of ultraviolet radiation on an oil-contaminated white paint, for example, is to accelerate the normal degradation rate of solar absorptance. We are certain that the reported poor - and often-times erratic - performance in space of many white coatings has been the direct result of contamination. We are convinced that the timely application of a protective coating to all exposed, critical thermal control surfaces, to be removed immediately prior to launch, should be made standard procedure. From the time that a coating is applied until the time of launch, the opportunities for contamination are virtually limitless. Since the effects of contamination are never desirable, the primary thrust of any R&D effort should be towards protection - at least until more fundamental studies of contaminants and their effects can isolate the sources and correct the conditions leading to contamination.

Contamination and its effects have been receiving a great deal of attention in the last two years. Large vehicle sizes and the increasing degree of sophistication in flight experiments and scientific instrumentation place strong demands upon the

cleanliness of spacecraft and spacecraft components. A wide array of environments will be experienced by the spacecraft on its way from the various manufacturers and assemblers of its components, to the launch site, and eventually into its space mission.

Attention is now being given to the effects of a salt-spray environment. What effects storage at Kennedy Space Flight Center, for example, may have on a paint's performance remains relatively unknown, although we have speculated with confidence that they are not good, especially if the salt-spray accumulation is significant.

Outgassing is still another form of potential contamination, and likewise has come under a lot of scrutiny. Outgassed vapors become contamination when they condense on a surface and interfere with the function of that surface. The fact that a material may outgas is not as important as the nature of the outgassed vapors and their effect on the surfaces upon which they condense. From an engineering standpoint the only criterion of contamination is a deleterious effect on affected surfaces. This is because the function of some surfaces is impaired by any condensation, however slight or whatever the condensed species. The outgassing problem, in terms of contamination, will always have to be confronted on a largely subjective basis.

4.2 Strippable Prelaunch Protective Coatings

4.2.1 General Remarks

The studies conducted under this program have sought to develop protective coatings for various, representative thermal control surfaces. We have chosen four representative surfaces: S-13G, Z-93, polished aluminum and suprasil quartz. While largely arbitrary these choices cover a large spectrum of actually used materials - from the silicones to the inorganic paint systems and from the metals to the dielectric surfaces. The ideal coating

would be an universal one; it would be water-based, impermeable, adherent to all surfaces, easily stripped even after long periods of outdoor exposure, readily identifiable as a protective coating, and, of course, would leave no contamination.

4.2.2 Test Conditions

The efficacy of the protective coatings was tested in several different ways, all of which, however, involved coating the substrate (S-13G, Z-93, etc.) with the protective coating, removing the latter after a predetermined period of contact, and then exposing the substrate to ultraviolet irradiation. If the "protected" substrate degraded faster than normal, the particular strippable coating would not be considered further. All samples were exposed in duplicate in the Weather-O-Meter test for a period of 335 hours, equivalent to approximately one year's atmospheric exposure. After the Weather-O-Meter test, two IRIF tests of Z-93 and S-13G coatings previously protected with strippable coatings were run. Four samples of Z-93 and four of S-13G were exposed to ~1300 ESH of ultraviolet radiation. The sample schedule, which was the same in both tests, was as follows: one unprotected sample was retained as a control: a protective coating was not applied, and the sample was stored in the lab; a second sample was coated with a protective coating and was also exposed only to the lab environment; a third sample was not given a protective coating but was exposed in the Weather-O-Meter (for 335 hrs); and the fourth sample was both coated and exposed in the Weather-O-Meter (335 hrs). In all cases Potter Paint's Formula No. ZM-11-CC was used over S-13G, and Goodrich #8 over Z-93. Goodrich #8 is an IITRI designation for the mixture: 60% Hycar 2679 and 40% Hycar 2600x138.

4.2.3 Test Results

The damage in test IRIF-I-47 was so severe that contamination was strongly suspected. In Table 6 we present for both IRIF-I-47 and IRIF-I-48 the induced spectral reflectance changes at 0.3875μ

Table 6

ULTRAVIOLET-INDUCED CHANGES IN
SPECTRAL REFLECTANCE OF "PROTECTED" PAINT FILMS

		<u>S-13G</u>	
		Induced Spectral Reflectance Changes, ΔR_{λ}	
<u>Protective Coating</u>	<u>Weather Exposure</u>	<u>I-47 (1300 ESH)</u>	<u>I-48 (1350 ESH)</u>
None	None	23.5	25.5
Potter	None	65.0(0.4)*	65.0(0.39)
None	335 hrs	21.5	25.0
Potter	335 hrs	39.0	59.5
Contact Time**		40	84
		<u>Z-93</u>	
None	None	7.5	4.5
Goodrich-8	None	14.0	10.5
None	335 hrs	7.5	4.0
Goodrich-8	335 hrs	13.0	---
Contact Time		40	84

*The peak of the curve of ΔR vs λ usually occurs at $\lambda = 0.3875\mu$; the number in parentheses is the wavelength (μ) at which the peak occurs when different from 0.3875μ .

**Contact time, number of days protective films were in contact with "protected" surfaces before being stripped for irradiation test.

(which for both S-13G and Z93 is the wavelength at which the spectral damage peaks). From this table one can easily observe several trends. First, coatings which were "protected" suffer much greater damage than those not protected. Second, the ultraviolet stability is not affected by a Weather-O-Meter exposure. Third, the time of contact between the strippable coating and the "protected" coating apparently affects the latter's ultraviolet stability. (Previous IRIF tests of surfaces with much less contact time did not exhibit unusual damage.)

Since we took considerable care in setting up Test I-48 to avoid any possible sources of contamination, we are reasonably certain that the data of that test are valid. The degradation of Z93 in IRIF-I-48 was slightly more than half that in Test I-47, and was within the normal range of degradation for a nominal 1300 ESH exposure. The S-13G samples, in both tests, degraded substantially more than expected, especially the control samples. The improvement in the performance of the Z93 control from test I-47 to I-48 was not accompanied by a similar improvement in the S-13G control. There are two possibilities: selective effects of the contaminant(s) on silicones, and excessive degradation to which the S-13G may have been predisposed by overgrinding. The first of these is more likely.

These tests have shown that the long term contact between the strippable coating and the surface it protects has a degrading effect. Earlier tests showed that contact times of similar but lesser duration did not affect the ultraviolet stability of S-13G.

A mitigating effect of the Weather-O-Meter exposure was noted. The degradation of "unprotected" samples exposed to the Weather-O-Meter was usually less than a "protected" but otherwise identically treated sample.

4.2.4 Conclusions

It appears that none of the protective coatings tested can be used with either Z-93 or S-13G. It may be possible to adjust formulations to achieve better initial adhesion characteristics, but the environmental stability of the "protected" surface will inevitably be a critical problem. We discovered that coating contact times of less than ~30 days result in no degradation, while contact times greater than this pre-dispose the "protected" coating to unusually severe ultraviolet radiation damage. The explanation for this is not clear.

4.3 Salt Spray Effects on S-13G

To gain some idea of what might happen to S-13G exposed over a long period of time to a salt-spray environment, we put a thick layer of simulated salt water (a saline solution containing representative amounts of the major constituents of ocean water) on the surface of several S-13G coatings and allowed them to evaporate to dryness. Four (4) S-13G coupons were prepared (from IITRI batch C-076); two were untreated and the other two treated as indicated above. The solar absorptance values before and after exposure to 1800 ESH in IRIF Test I-41 are shown in Table 7.

Table 7

RESULTS OF SIMULATED SALT SPRAY EXPOSURE EFFECTS ON S-13G UV DEGRADATION

No.	Sample Description	Solar Absorptance		
		Initial	Final*	$\Delta\alpha_s$
1	S-13G Control	0.204	0.248	0.044
2	S-13G with Salt Spray	0.202	0.256	0.054
3	S-13G Control	0.204	0.238	0.034
4	S-13G with Salt Spray	0.205	0.243	0.039

*After exposure to 1800 ESH of AH-6 radiation.

In general, the salt spray samples degrade only slightly more than standard S-13G. Surprisingly, the S-13G with visually noticeable amounts of salt water deposits did not degrade as much as might be expected. The spectral data (see Figure 36) indicate that the spectral degradation is characteristic of S-13G. It thus appears that a salt spray environment only slightly increases the susceptibility to solar radiation damage - at least, for S-13G. The same results were obtained when essentially the same test was repeated in IRIF-I-44, in which the exposure was 342 ESH. The $\Delta\alpha_s$ values for the control and salt-spray S-13G samples were 0.024 and 0.015, respectively. The control sample degradation is higher than expected, making these particular data

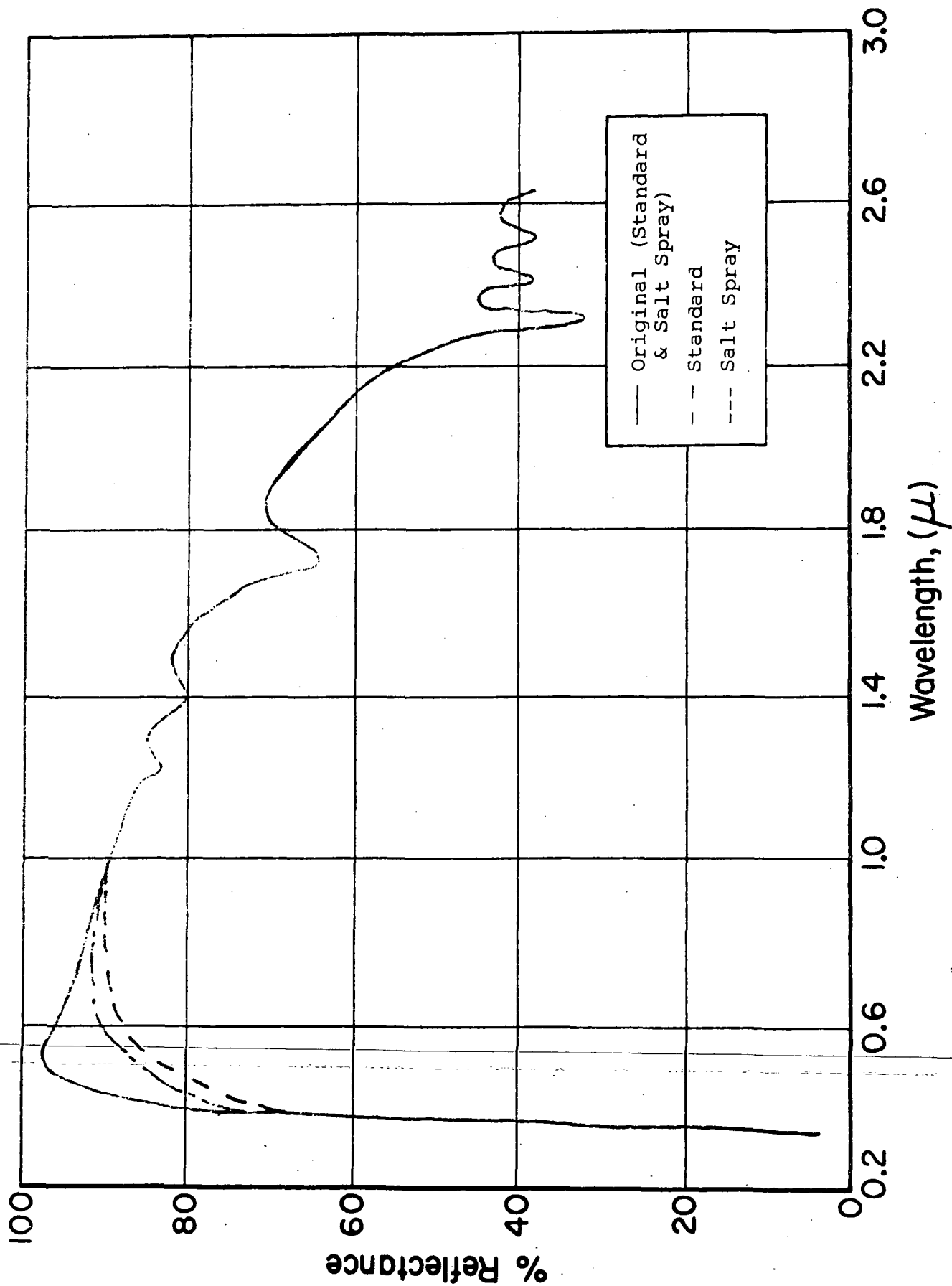


Figure 36 . UV-DEGRADATION OF STANDARD AND SALT SPRAY TREATED S-13G

somewhat questionable. Assuredly, however, the effect of a build-up of simulated ocean spray is minimal, if not within the nominal range of degradation.

4.4 Ultraviolet Stability of Low Outgassing S-13G

As reported in a previous Triannual Report (Ref. 1), a series of modified S-13G paint samples were prepared. These modified paints were formulated according to standard S-13G specifications, using RTV 602 silicone which had previously been thermally treated to remove low molecular weight components.

IRIF Test I-46 was devoted to testing the ultraviolet resistance of coatings made from "stripped" RTV 602. Reflectance measurements were made after 1000 ESH and after 2250 ESH. Figure 37 is well representative of all the spectra. With one minor exception all twelve samples performed almost exactly alike. The conclusion is that vacuum stripping of RTV 602, regardless of how it is accomplished, does not affect the ultraviolet stability of the silicone polymer or the coatings made from it. This confirms the same results obtained previously under a different program (Ref. 8). Table 8 lists the polymers from which the tested S-13G paints were made, and the spectral reflectances of the latter at several visible wavelengths.

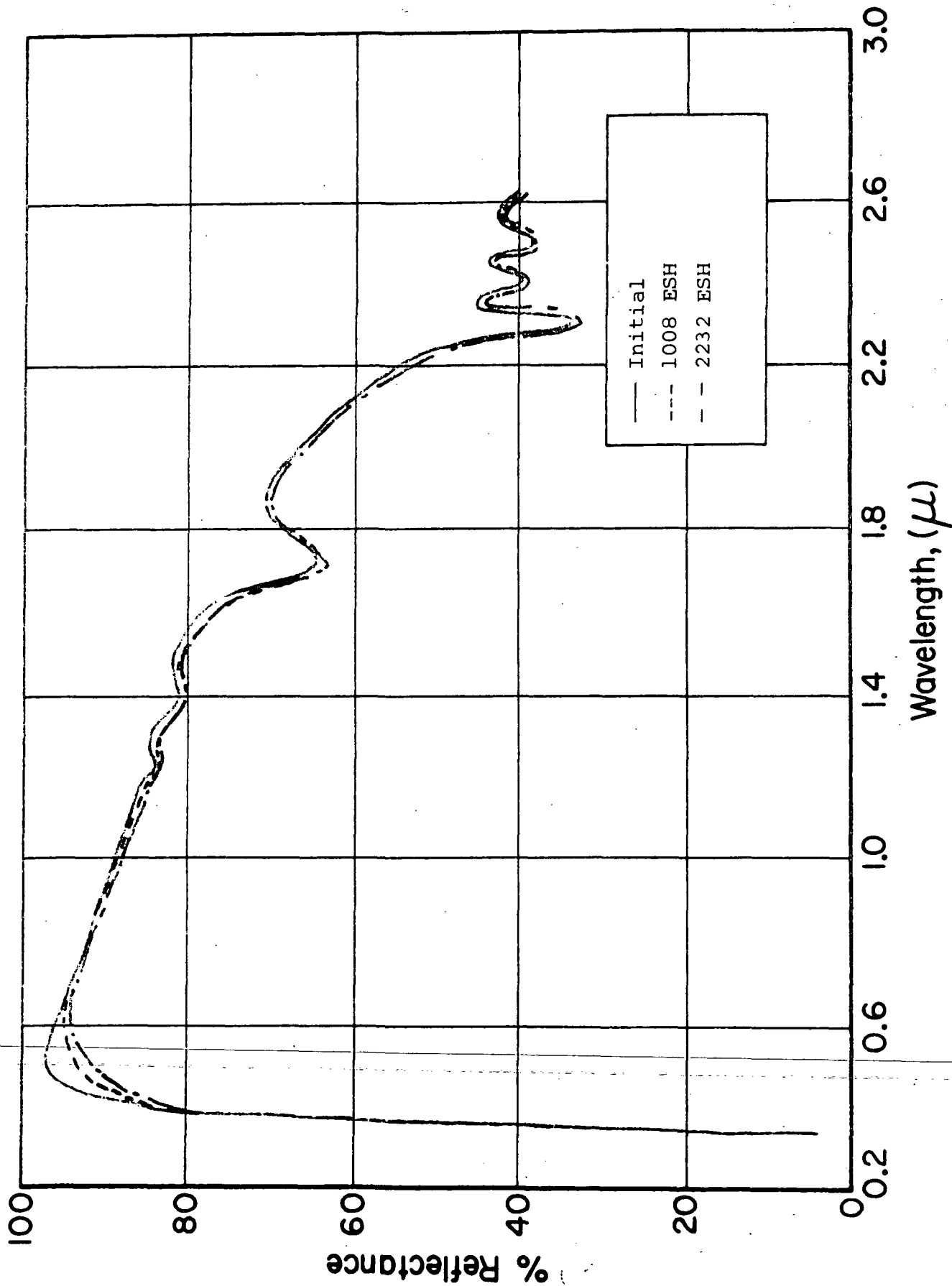


Figure 37 EFFECT OF UV IRRADIATION ON "STRIPPED" S-13G

UV IRRADIATION PERFORMANCE OF "STRIPPED" S-13G

No.	Description	ESH:	Spectral Reflectance Values											
			400 nm			500 nm			600 nm			700 nm		
			0	1000	2250	0	1000	2250	0	1000	2250	0	1000	2250
1	GSFC* - 11		68.9	65.5	58.7	87.1	85.5	81.8	88.0	87.1	84.6	87.2	81.4	85.0
2	GSFC* - 11		69.3	65.8	-----	86.7	85.0	-----	87.1	86.1	-----	86.2	86.0	-----
3	J.B.** No. 4		71.3	67.6	60.0	89.5	87.8	83.6	91.3	90.2	88.5	90.3	90.1	89.0
4	J.B.** No. 4		71.5	64.5	60.6	89.7	87.8	84.2	91.0	90.2	88.4	90.2	90.1	89.0
5	J.B. No. 5		72.9	66.9	60.9	90.3	87.8	84.5	91.7	90.9	89.3	91.2	90.5	90.0
6	J.B. No. 5		69.0	62.0	57.7	89.7	85.9	82.3	91.6	90.2	88.3	91.5	90.6	89.7
7	J.B. No. 6		72.2	66.9	61.5	89.7	86.7	84.2	90.1	89.0	87.8	89.0	88.5	88.2
8	J.B. No. 6		72.8	67.0	-----	90.0	86.9	-----	90.2	89.0	-----	90.3	88.5	-----
9	J.B. No. 7		72.8	67.1	63.5	91.0	87.8	85.7	92.2	90.4	89.9	91.8	90.8	90.2
10	J.B. No. 7		73.3	65.0	63.0	90.8	87.7	85.2	92.2	90.6	89.6	91.8	91.0	90.0
11	J.B. No. 8		72.4	66.8	63.0	91.2	87.9	85.9	92.6	91.9	89.7	91.9	91.0	90.0
12	J.B. No. 8		73.9	69.0	-----	92.0	89.3	-----	93.0	91.9	-----	92.8	97.0	-----

*Polymer prepared by Dr. Ben Seidenberg at NASA-GSFC using pot distillation.

**All "J.B." polymers prepared by ITRI by molecular distillation.

REFERENCES

1. Gilligan, J.E., "Development of Space Stable Thermal Control Coatings for Use on Large Space Vehicles," IITRI Report No. C6233-4 (Triannual Report) May 15, 1971.
2. Zerlaut, G.A., Gilligan, J.E. and Ashford, N.A., "Space Radiation Environmental Effects in Reactively Encapsulated Zinc Orthotitanates and Their Paints," AIAA Paper No. 71-449, Presented to the AIAA 6th Thermophysics Conference, Tullahoma, Tennessee, April 26-28, 1971.
3. Gilligan, J.E. and Ashford, N.A., "Development of Space Stable Thermal Control Coatings for Use on Large Space Vehicles," IITRI Report No. C6233-8 (Triannual Report), October 15, 1971.
4. Gilligan, J.E. and Zerlaut, G.A., "Development of Space-Stable Thermal-Control Coatings," IITRI Report No. U6002-90 (Triannual Report), July 1, 1970.
5. Tompkins, E.H., "Stable White Coatings," Armour Research Foundation Report No. ARF 3207-5 (Interim Report), 13 April 1962.
6. Nygaard, K.H., "Instrumental Problems Related to the Measurement of Quantum Efficiency of Sodium Salicylate," JOSA 55, (8), pp. 944-46, Aug. 1965.
7. Allison, R., Burns, J., and Tuzzolino, A.J., "Absolute Fluorescent Quantum Efficiency of Sodium Salicylate," JOSA 54, (6), pp. 747-51, June 1964.
8. Gilligan, J.E. and Rogers, F.O., "Development and Manufacture of a Special S-13G Paint Coating," IITRI Report No. C6227-1 (Final Report), Dec. 17, 1970.